Polymer Chemistry

Light and Latex: Advances in the photochemistry of polymer colloids

Journal:	*Polymer Chemistry*
Manuscript ID	PY-REV-03-2020-000349.R1
Article Type:	Review Article
Date Submitted by the Author:	01-May-2020
Complete List of Authors:	Scott, Philip; Virginia Polytechnic Institute and State University, Macromolecules Innovation Institute; Virginia Polytechnic Institute and State University, Department of Chemistry Kasprzak, Christopher; Virginia Polytechnic Institute and State University, Department of Chemistry; Virginia Polytechnic Institute and State University, Macromolecules Innovation Institute Feller, Keyton; Virginia Polytechnic Institute and State University, Department of Mechanical Engineering; Virginia Polytechnic Institute and State University, Macromolecules Innovation Institute Meenakshisundaram, Viswanath; Virginia Polytechnic Institute and State University, Department of Mechanical Engineering; Virginia Polytechnic Institute and State University, Macromolecules Innovation Institute Williams, Christopher; Virginia Polytechnic Institute and State University, Department of Mechanical Engineering; Virginia Polytechnic Institute and State University, Macromolecules Innovation Institute Long, Timothy; Virginia Polytechnic Institute and State University, Department of Chemistry; Virginia Polytechnic Institute and State University, Macromolecules Innovation Institute

REVIEW

Light and Latex: Advances in the photochemistry of polymer colloids

Received 00th January 20xx,
Accepted 00th January 20xx

DOI: 10.1039/x0xx00000x

Philip J. Scott,[a] Christopher R. Kasprzak,[a] Keyton D. Feller,[b] Viswanath Meenakshisundaram,[b] Christopher B. Williams[b], and Timothy E. Long*[a]

Unparalleled temporal and spatial control of colloidal chemical processes introduces immense potential for the manufacturing, modification, and manipulation of latex particles. This review highlights major advances in photochemistry, both as stimulus and response, to generate unprecedented functionality in polymer colloids. Light-based chemical modification generates polymer particles with unique structural complexity, and the incorporation of photoactive functionalities transforms inert particles into photoactive nanodevices. Latex photo-functionality, which is reflected in both the colloidal and coalesced states, enables photochromism, photoswitchable aggregation, tunable fluorescence, photoactivated crosslinking and solidification, and photomechanical actuation. Previous literature explores the capacity of photochemistry, which complements the rheological and processing advantages of latex, to expand beyond traditional coatings applications and enable disruptive technologies in critical areas including nanomedicine, data security, and additive manufacturing.

1. Introduction

The design and application of latex, colloidal dispersions of polymer particles in water, endures as an immense field of innovation throughout academia and the industrial sector. The allure of these colloids lies in the unique benefits they offer for polymerization conditions, facile processing, and modular modification of polymeric materials.[1] Centered on coating and adhesive applications, polymer latex currently comprises a multi-billion-dollar global industry.[2,3] While nature provided the first example of these materials in the form of natural rubber latex, developments in emulsion polymerization and emulsification processes have broadly expanded the compositions, morphologies, and functionalities of latexes beyond polyisoprene.[4] The incorporation of light-based processes further revolutionizes these materials, yielding unparalleled synthetic capability and functional responsivity to polymer colloids.

Photochemistry affords unique spatial and temporal control to synthetic and modification processes. Light is currently the fastest mode of energy and stimulus delivery, offering precise selectivity across the electromagnetic spectrum, and is readily shaped and modulated with currently available optics technology. In latex, photochemistry enables the precise manufacturing, modification, and manipulation of microscopic polymer particles to revolutionize the expansive reach of the latex industry and introduce new possibilities for these materials in fields such a biological tracking, drug delivery[5–7], data storage and security[8,9], and additive manufacturing.[10–12] Herein we explore leading examples of the unique compositions and functionalities available through the synergistic merging of latex and photochemistry.

Emulsion polymerization stands as a leading method for synthesizing latex polymer colloids. This approach typically involves a free radical polymerization of hydrophobic monomer emulsified in water with amphiphilic surfactant molecules or co-monomers. Other routes to fabricating polymer colloids include suspension[13] and dispersion[14] polymerizations[15] in addition to the emulsification of preformed polymer solutions[16] or melts.[17] Photopolymerization in dispersed systems represents an important and heavily studied area of research. A recent review by Jasinski *et al.* provides an exhaustive summary of the advancements on this subject,[18] and recent investigations by Jasinski *et al.* demonstrate multiple examples of the state-of-the-art for latex photopolymerization.[19–22] Therefore, this review focuses on the other roles of light in latex, specifically photochemical modification and photoactivated response. This review encompasses examples of these light-driven processes performed in both the liquid colloidal state and the dried, coalesced film state.

2. Photomodification of Latex

A plethora of well-known photoinitiated coupling and polymerization reactions, commonly used for the synthesis and modification of polymers, offer a unique capability to alter and access new particle structures and compositions in latex. Light-based augmentation of polymer colloids focuses primarily on chemical modification, which provides stimuli-responsivity or intraparticle photocrosslinking, to improve the mechanical properties of the resultant film after drying and particle coalescence.

---

[a] *Department of Chemistry, Macromolecules Innovation Institute, Virginia Tech, Blacksburg, VA 24061*
[b] *Department of Mechanical Engineering, Macromolecules Innovation Institute, Virginia Tech, Blacksburg, VA 24061.*

2.1 Intraparticle photocrosslinking

Thiol-ene chemistry is a prevalent click reaction, which involves the radical-driven attachment of thiol functional groups to alkenes.[23] Thiol-ene chemistry offers an alternative to traditional sulfur-based crosslinking (vulcanization), enabling similar attachment of polydiene chains with increased control of initiation and kinetics with significantly less toxic reagents.[24] Schlögl and coworkers introduced "photo-vulcanization" of natural rubber (polyisoprene) latex using photoinitated thiol-ene chemistry.[24–26] The addition of a radical photoinitiator and multifunctional thiol crosslinker within the latex particles enabled photo-activated thiol-ene crosslinking upon exposure with ultra-violet (UV) light. Light-based processes in latex are inherently difficult as these heterogeneous systems typically contain nano- or micro-scale particles. Latex particles scatter wavelengths similar to and smaller than their size (typically in the UV-visible range) and therefore decrease the depth that incident light effectively penetrates the colloid.[27,28] A specialized "falling film" reactor irradiated a thin film of liquid latex, enabling a continuous reaction process, which mitigated these depth of penetration concerns.[26,29] Shown in Fig. 1, photocrosslinking in the colloidal latex state induced intraparticle photocrosslinking and yielded a "prevulcanized" liquid colloid containing internally crosslinked, discrete polymer particles in water. Upon drying, these particles coalesced and entangled to yield a film with crosslinked regions connected via physical entanglement of the remaining uncrosslinked chains. Thus, this approach did not provide long-range crosslinking throughout the film, which limited mechanical strength and solvent resistance. In this regard, the authors also demonstrated (with the same chemistry) film-state UV exposure, which extended photocrosslinking globally throughout the film rather than a particle-by-particle basis. Other film-state photocrosslinking strategies will be discussed in greater detail later in this review (Section 3.7.1).

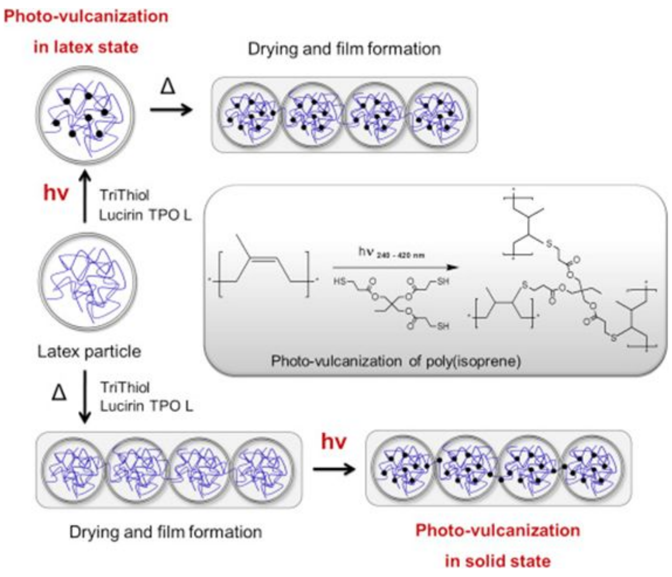

Fig. 1 Photo-induced crosslinking of natural rubber latex in both latex- and film-states investigated by Schlögl and coworkers. Copyright 2014. Reprinted with permission from Elsevier from reference 24.

While thiol-ene chemistry provides an interesting analog to sulfur vulcanization of diene rubbers, the presence of thiols incurs undesirable odors, which may not be suitable for certain applications requiring human exposure. Work by Wiroonpchit and coworkers investigated an alternative approach to intraparticle photocrosslinking of natural rubber latex with diacrylates instead of thiols.[30,31] It is interesting to note that both Schlögl and Wiroonpchit observed only minor inhibition by oxygen regardless of atmospheric conditions. While the former example employed thiol-ene chemistry, which is an oxygen-resistant click reaction, the use of acrylate chemistry implied an additional effect to explain this insensitivity. Schlögl *et al.* suggested that the decreased surface area-to-thickness ratio in their reactor compared to thin film cases (which displayed oxygen inhibition) may limit oxygen accessibility to photoinitated radicals.[26]

Other efforts investigated more unique chemistries for photocrosslinking beyond traditional photoinitated radical approaches. Coumarin[32–34] and cinnamate[35,36] functional groups enable "initiator-free" photocrosslinking via coupling reactions in response to UV light. Shi and coworkers designed novel latexes containing cinnamate functional groups within the polymer backbone. The reversible nature of the 2+2 cycloaddition of cinnamates enabled photo-selective crosslinking and decrosslinking within the latex particle, which resulted in controllable changes in polymer particle diameter.[37] Albuszis *et al.* introduced photo-induced azide-to-nitrene decomposition as a novel method for intraparticle photocrosslinking.[38] As shown in Fig. 2, pendant azide moieties decomposed to reactive nitrenes in response to UV light;

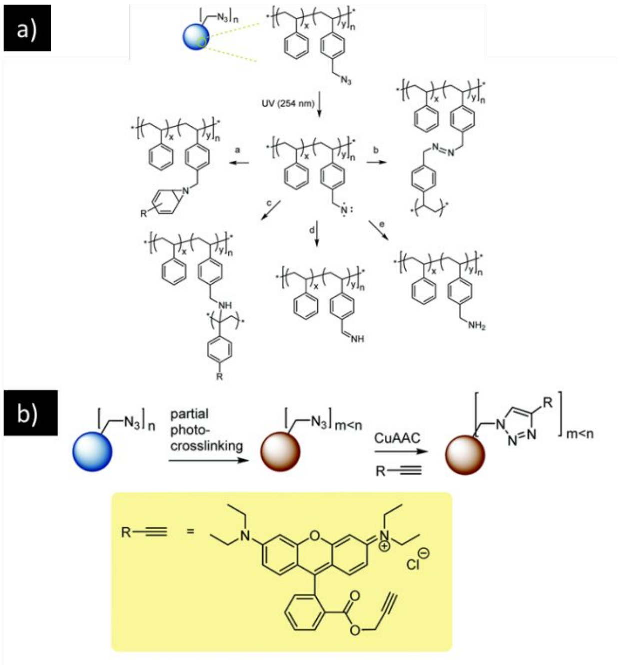

Fig. 2 Albuszis *et al.* investigated (a) photo-induced azide-to-nitrene reactions which enable photocrosslinking within polymer particles. (b) Azide-alkyne click reactions of residual azides enables subsequent ligation of particle polymers. Copyright 2016. Reproduced from reference 38 via Creative Commons License (CC BY-NC 3.0). Published by the Royal Society of Chemistry.

these groups undergo a variety of reactions, many of which lead to chain-chain crosslinking. Subsequent azide-alkyne click reactions with unconsumed azides enabled ligation of functional molecules to the particles, a direction of latex modification discussed in the next section.

2.2 Photochemical ligation, grafting, and attachment

Photolabile coupling reactions demonstrate unique promise for the synthesis of grafted and functionalized surfaces[39,40] as well a new route to more complex polymer architectures.[41–44] For polymer latex, these techniques offer unique tunability and access to novel particle structures and reactivities. Analogous to the functionalization of inorganic nanoparticles, both “grafting-from” and “grafting-to” techniques enable the synthesis of “hairy” latex particles. For the former, polymer chains are grown from the surface of the particle as a surface-initiated polymerization. In the latter case, preformed polymer chains are attached to the surface of a particle, typically through click coupling reactions.

2.2.1 Photochemical grafting-from modification of latex Illustrated in Fig. 3, work in the Ballauf group investigated the photo-initiated grafting-from of polyelectrolyte brushes from the surface of polystyrene latex particles.[45] Guo *et al.* described the synthesis of polystyrene (PS) cores via a conventional batch emulsion polymerization (Step 1).[45,46] After formation of the PS particles, the authors fed a polymerizable photoinitiator into the reactor to generate a photoinitiator shell on the surface of each particle. The photoinitiator was fed slowly (Step 2) in “starved” semibatch conditions (slower than the rate of polymerization) to ensure the addition of functional shells on existing particles rather than the formation of new particles. This photo-functional latex was then charged into a UV reactor with acrylic acid and irradiated to polymerize poly(acrylic acid) (PAA) brushes from the particle surfaces.

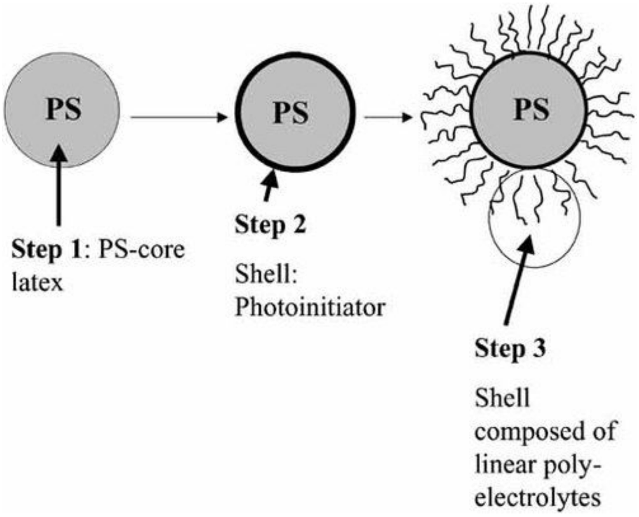

Fig. 3 Guo *et al.* investigated photo-induced, surface-initiated grafting-from polymerization of polymer “hairs” onto polystyrene latex particles. Copyright 2003. Reproduced with permission from John Wiley & Sons, Ltd from reference 45.

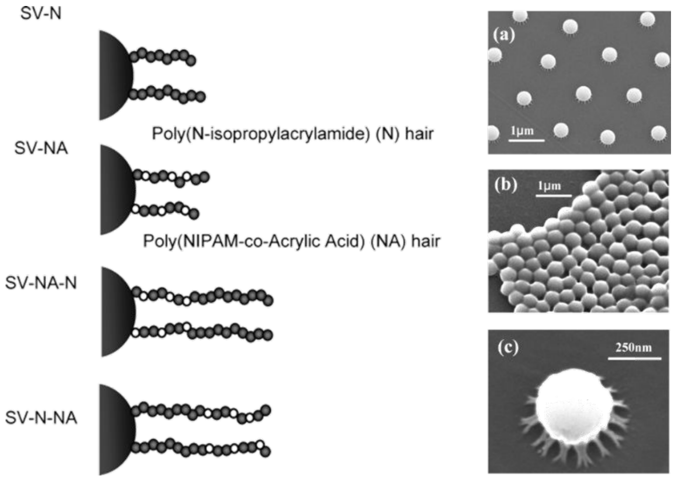

Fig. 4 Tsuji and coworkers designed copolymer functionalized latex particles by photoiniferter controlled radical polymerization from the surface. Copyright 2004. Adapted with permission from the American Chemical Society from reference 47.

These modified latex particles exhibited stimuli-responsive colloidal stability to both pH and salt concentration of the aqueous phase due to the pH labile ionizability of PAA.

Tsuji *et al.* introduced grafting-from via the *controlled* radical polymerization from latex surfaces.[47] The authors described the synthesis of poly(styrene-*co*-vinylbenzyl chloride) latex particles via soap-free emulsion polymerization. Covalent attachment of a photoiniferter to the surface via a post-polymerization substitution reaction provided photo-reactive latex particle substrates. Upon UV exposure, this iniferter produced a surface-bound radical, which initiated the grafting-from polymerization of “hairs” from the particles. Shown in Fig. 4, the “living” nature of this controlled radical polymerization enabled the formation of *block* copolymer hairs, unattainable by the free radical grafting techniques described previously. Copolymer hairs of N-isopropylacrylamide (NIPAM) and acrylic acid (AA) provided responsivity to temperature, pH, and ionic strength stimuli.

Although not a modification technique, it is important to highlight the capability of polymerization-induced self-assembly (PISA) techniques to produce colloidal polymer particles with tailored “hairy” surface chemistry in a direct synthetic approach.[48,49] Multiple examples show the promise of photopolymerization to generate unique polymer particles through photo-PISA strategies.[50–54]

2.2.2 Photochemical “grafting-to” modification of latex As discussed previously, thiol-ene chemistry is a radical-driven coupling reaction made photoactive with the use of a radical photoinitiator. Beyond photocrosslinking, this click reaction is ideal for grafting-to applications due to its high efficiency, lack of side products, and resistance to oxygen inhibition.[23] Yang and coworkers described the utilization of reversible addition-fragmentation chain transfer (RAFT) polymerization in both miniemulsion and homogenous solution conditions to synthesize “click ready” latex particles and polymer “hair” ligands, respectively.[55] Illustrated in Fig. 5, the authors synthesized amphiphilic diblock copolymers PAA-b-Poly(n-butyl acrylate-*co*-cyclohex-3-enylmethyl acrylate) via RAFT polymerization to serve as both surfactants and macro-chain transfer agents (macro-CTA) for miniemulsion RAFT polymerization of styrene latex particles. RAFT polymerization from the hydrophobic end of these reactive

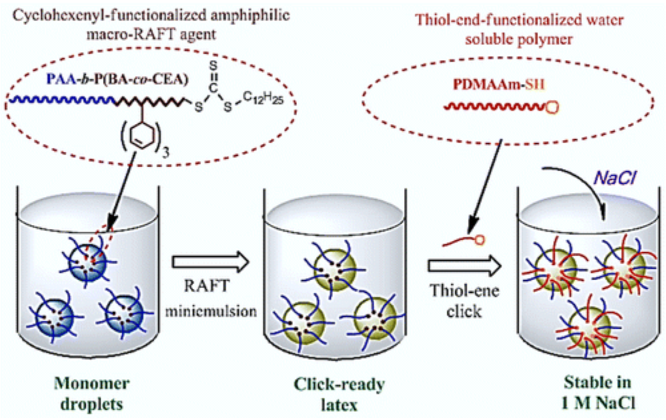

Fig. 5 Yang et al. developed hairy latex particles via thiol-ene "grafting-to" of thiol-functionalized polymer chains to surface-bound alkenes. Copyright 2015. Reproduced with permission from the American Chemical Society from reference 55.

surfactants yielded polystyrene latex particles with surfaces decorated in a covalently attached alkenes (CEA repeating units).

RAFT polymerization also generates chains with thiocarbonate end groups. Facile cleavage of these groups with amines yields primary thiol endcaps, converting the polymer chains into "clickable" ligands. The authors irradiated a mixture of the thiol end-capped polymer, the alkene-functionalized latex particles, and a radical photoinitiator to complete the photochemical grafting-to ligation via thiol-ene click chemistry. The authors reported significant increases in colloidal stability with respect to salt concentration. Recent work by Huang *et al.* explored a similar synthetic approach to fabricate biotin-functionalized poly(methyl methacrylate) PMMA latex spheres which immobilized fluorescein isothiocyanate streptavidin via strong non-covalent interactions.[56] As a result, the authors show promise of photo-functionalized latex for biomedical applications including immunofluorescent staining.

Recent work from the Barner-Kowollik and Bowman groups explored wholly different chemistry for photochemical grafting-to latex ligation: nitrile imine-mediated tetrazole-ene cycloaddition (NITEC)[57,58] and nitrile imine carboxylic acid ligation (NICAL).[57] Fluorescent pyrazoline linkages, consequent of the coupling reactions, yielded fluorescent polymer particles; a heavily studied latex photo-response which will be discussed later in this review.

3. Photoresponsive & Photoactive Latexes

Stimuli-responsive polymer latexes remain a major topic of investigation due to their unique combination of ideal processing and controllable function. Common target stimuli include temperature[59,60], pH[61], and gas exposure.[62,63] In particular, photochemical response represents a major focus in this area, however, as mentioned previously, the same colloidal structure that provides advantageously low viscosities and high surface areas for polymer colloids also results in light scattering.[27,28] However, developments in processing techniques, reactor designs[26,29,64], and even 3D printer designs[10] allow for the mitigation of deleterious scattering to provide access to the unique advantages that result from the combination of light-driven processing and latex. This section highlights major advances in the design of photoresponsive and photoactive latex, covering response in both the liquid colloidal state and coalesced film state.

Photochemistry finds use throughout both traditional and novel applications of polymer latex. Coatings comprise a major portion of the latex industry, and most encounter light exposure in some form during their application. Photoactive latexes therefore offer an opportunity to harness or mitigate this incident energy source. While considerable efforts center on UV-absorption to protect substrates beneath the coating, other strategies utilize ambient light for film-state photocrosslinking. The colloidal morphology of latex particles provides unique opportunities for photoresponsive behavior more complex than film-state photocrosslinking. More recent developments investigate the incorporation of photoactive molecules to access novel latex properties such as fluorescence, photochromism, photomechanical deformation, and colloid-state photocuring to reenvision polymer latex particles as functional nanomaterials.

3.1 Light absorbance and photochromism in latex

Molecular photoactivity is founded upon absorption, which by itself is an area of critical research for many applications that demand controlled color or UV protection. The direct mixing of dyes and pigments into latex represents a common approach to alter the absorption of latex, primarily for the fabrication of colored paints and coatings. However, more intricate approaches to controlling light absorbance and improving color "fastness" (solvent resistance) in latex include the covalent incorporation of reactive dyes into the polymer chains by copolymerization during emulsion polymerization. The resultant "covalently-colored" latexes exhibit significantly lower dye migration and leachability (compared to those with unbound, free dyes), yielding more resilient coloration.[65–68] In addition to coloration, other strategies, target UV resistant and protective coatings through the incorporation of absorbing functional groups[69,70] or inorganic fillers[69–74] (as demonstrated by Aguirre *et al.* in Fig. 6) into the latex.

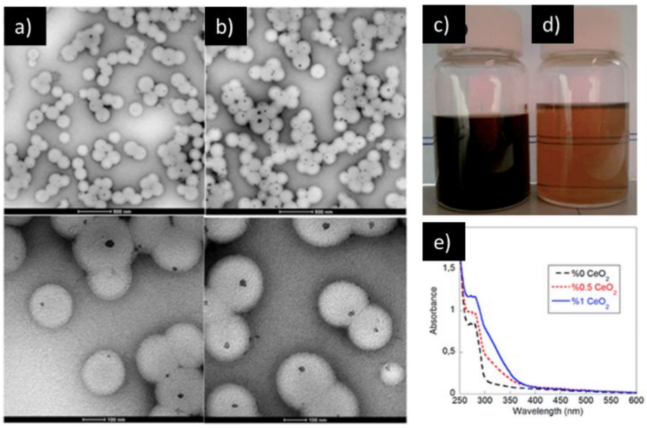

Fig. 6 Aguirre et al. incorporated UV-absorbing CeO2 nanoparticles into latex via miniemulsion polymerization. (a&b) TEM micrographs of hybrid latexes. (c & d) CeO2 dispersions in solvent and monomer, respectively. (e) UV absorption of films containing various CeO2 concentrations. Copyright 2013. Reproduced with permission from the Royal Society of Chemistry from reference 71.

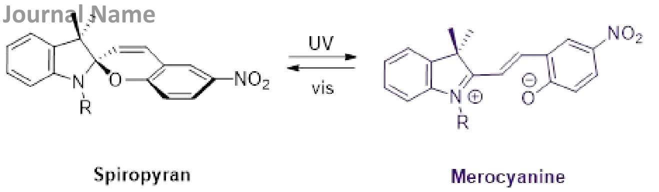

Scheme 1. Photoactivated, reversible photoisomerization of spiropyran to colored, ring-opened merocyanine isomer.

In contrast to work by Aguirre et al., Martín-Fabiani et al. investigated the incorporation of nanoceria into polymer latexes as Pickering dispersions and hybrid mixtures of latex particles and ceria sol, as a result, the ceria was observed to align in a "honeycomb" structure at particle interfaces during coalescence.[75]

Photochromism describes the ability of a molecule to switch its absorbance spectrum in response to a light stimulus.[76] A widely popular photochromic compound, spiropyran (SP), serves as a highly versatile "molecular switch", and affords light-based control of chemical processes for a plethora of applications.[77,78] Shown in Scheme 1, spiropyran undergoes a reversible photoisomerization to an open-ring form (merocyanine) in response to UV light (365 nm) which reverses spontaneously or more rapidly upon exposure to visible light.[79]

Incorporation of spiropyran into latex typically occurs either as a small molecule additive[8] or via emulsion copolymerization with a reactive derivative of the photoactive molecule[9,80–82] Su *et al.* provided an early example of this approach through the synthesis and miniemulsion copolymerization of a modified spiropyran methacrylate monomer. The resultant latex exhibited reversible photochromism over multiple cycles by altering exposure with visible and UV light. Shown in Fig. 7, Abdollahi and coworkers investigated a similar approach through the synthesis and copolymerization of an acrylate-functional spiropyran monomer (SPEA) with methyl methacrylate (MMA).[81] The latex also possessed epoxide groups, via copolymerization with glycidyl methacrylate (GMA), which enabled covalent attachment to cellulose substrates for photoactive coatings on paper.[83,84] The resultant latex exhibited reversible photochromism in both the colloidal and film/coating states. Work from the same group by Khakzad *et al.* expanded the use of spiropyran functionalized latex to investigate systems responsive to light, pH, and CO$_2$.[82]

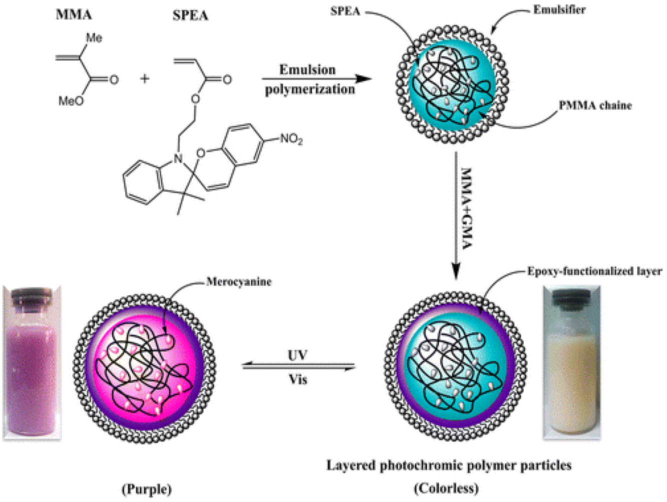

Fig. 7 Abdollahi and coworkers synthesized functionalized photochromic latexes, which display reversible photo-activated pigmentation in both colloidal (a) and film/coating states (b). Copyright 2015. Reproduced with permission from the American Chemical Society from reference 81.

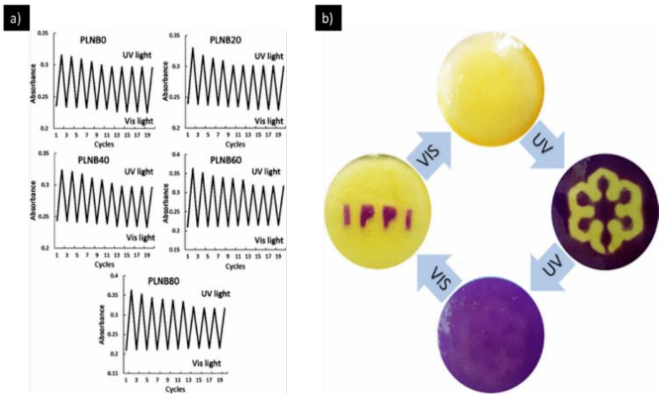

Fig. 8 Sharifian *et al.* investigated the application of reversibly photochromic latex films for optical data storage. (a) Reversible photochromism over multiple exposure cycles of visible and UV light. (b) Spatially selective photo-switching enables the creation of optical patterns in photochromic films. Copyright 2017. Reproduced with permission from the American Chemical Society from reference 9.

Shown in Fig. 8, Sharifian *et al.* investigated the application of films formed from photochromic latex for optical data storage.[9] Because the absorbance spectrum of spiropyran is wavelength dependent and reversible, the authors demonstrated the ability to print patterns on their surfaces, which were subsequently erased and rewritten over multiple cycles. Other exciting applications of these materials include anti-counterfeiting coatings for currency and sensitive documents.[84,85]

3.2 Luminescence and latex

Beyond absorbance, significant work investigates the *emission* of light by latexes. Fluorescence, rapid luminescence via light excitation,[86] represents a massively researched photoresponse for latex.[87–90] Extensive investigation proves the promise of fluorescent polymer nanoparticles as trackable molecular probes. These provide unique insight into complex processes including cellular uptake,[33,91–95] fluid dynamics and flow tracing,[96,97] "hard sphere" atomistic models,[98–100] and drug delivery.[101] Further, in both colloidal and film states, fluorescent latexes enable next-generation technologies such as cell/tissue imaging, [5,92–94,101] smart coatings, fluorescent paint,[88,102] anti-counterfeiting and document security coatings,[84,85] optical data storage,[9,80,92] and optical logic gates.[103]

The inclusion of fluorescent molecules into polymers lends their functionality to a wide variety of materials. Common fluorescent moieties incorporated into latex include spiropyran,[80,81,83,84,87,91,104–107] coumarin derivatives,[33,93] dipyrromethene boron difluoride (Bodipy),[108] pyrozolines,[109] nitrobenzo-2-oxa-1,3-diazol (NBD),[98–100] tetraphenyl ethylene (TPE),[88,89] and azocarbazole (AzoCz) derivatives.[92,103,110] Incorporation of fluorophores can occur through the physical entrapment of small molecules[89,90,93,96,111–114] or quantum dots[101,115,124,116–123] within particles or at their surface. Miniemulsion polymerization is ideal for this strategy as the preforming of emulsion droplets mitigates concerns of fluorophore transport through water during particle synthesis. As discussed earlier, radically polymerizable derivatives of fluorophores enable the covalent attachment of these moieties to the polymer backbone within the particle via copolymerization.[80,81,105,108,110,125–127,83,85,87,92,98–100,103]

3.2.1 Spiropyran-functional latexes for photo-switchable fluorescence. As discussed previously, spiropyran provides photo-switchable absorption (photochromism) and has been extensively investigated in latex systems. Interestingly, this versatile molecule also provides photo-switchable fluorescence via the same reversible, photoisomerization from the nonfluorescent ring-closed spiropyran isomer to the fluorescent transoid ring-opened merocyanine isomer.[77] As a result, the fluorescence of spiropyran is selectively turned on or off. However, this property is strongly dependent on environment, staging an ideal opportunity for latex. Zhu and coworkers investigated the copolymerization of an spiropyran-acrylate derivative to yield functional latex particles via copolymerization with styrene, MMA, and n-butyl acrylate (BA) and compared these with analogous polymers in homogenous solution.[125] In solution (toluene), neither the spiro- or mero- isomers exhibited appreciable fluorescence. However, when incorporated into a polymer latex particle, the mero-isomer strongly fluoresced. The authors attribute this to the hydrophobic environment of the particle interior, which prevented nonradiative decay or electron-transfer pathways with solvent molecules and possibly provided restriction to rotational mobility within SP, which benefits fluorescence. Later work by Zhu and coworkers found further evidence of this effect of nanoenvironment on spiropyran fluorescence.[91] In spiropyran-functionalized poly(caprolactone) (PCL) particles, both the spiro- (green) and mero- (red) isomers strongly fluoresced at an excitation wavelength of 420 nm, rather than just the mero- form in the styrenic/acrylic latexes.

Traditional fluorescent molecules often exhibit decreased fluorescence at high concentrations due to the aggregation caused quenching (ACQ) effect.[128] Illustrated in Fig. 9, Li and coworkers developed a novel system to mitigate this effect by ionically attaching the fluorophores to the surface of latex particles, which separated the molecules and reduced their ability to aggregate.[102] The model fluorophore, rhodamine B, is ionizable and contains both negatively and positively charged moieties, dependent on pH. The authors synthesized latex particles with both positively and negatively charged surfaces to investigate attachment in different environments. Studies of the effects of particle size, rhodamine B concentration, and particle concentration on fluorescent properties found the ionically bound fluorescent systems to effectively overcome ACQ.

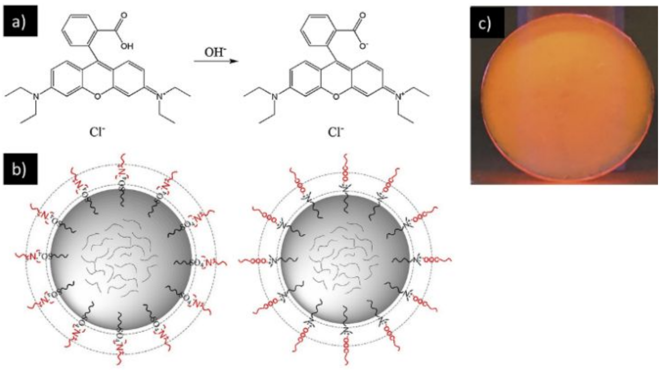

Fig. 9 Li et al. investigated the ionic attachment of rhodamine B (a) to the surface of anionically and cationically charged latex particles (b) to reduce aggregation caused quenching (ACQ) in the resultant films (c). Copyright 2018. Reproduced with permission from Elsevier from reference 91.

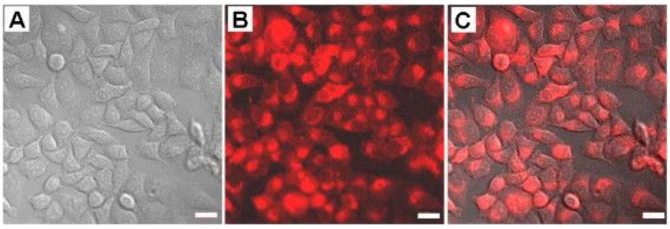

Fig. 10 Liu et al. imaged A549 cells with AIE-functional crosslinked polystyrene "dot" latex particles. Scale bar = 20 μm. Copyright 2014. Reproduced with permission from Elsevier from reference 132.

3.2.2 Aggregation-induced emission (AIE) in latex Another solution to ACQ arrived in the form of aggregation-induced emission (AIE) luminogens, which exhibit *stronger* emission at higher concentrations.[129] In sum, this is primarily due to physical confinement of intramolecular bond movement. Their advent by Tang *et al.* in 2001 launched a major wave of innovation in fluorescence technology, particularly for biological probes.[130] Zhang *et al.* created a radically polymerizable AIEgen for the facile creation of fluorescent polymer nanoparticles via emulsion polymerization with styrene and acrylic acid.[131] Shown in Fig. 10, Liu and coworkers developed a difunctional AIE crosslinker for the emulsion polymerization of luminescent crosslinked "dots", which exhibited strong red fluorescence and promising results for cell imaging.[132] Cao *et al.* report miniemulsion polymerization with the AIEgen, 1-allyl-1-methyl-2,3,4,5-tetraphenylsilole (AMTPS), also for cell staining and imaging applications.[133,134]

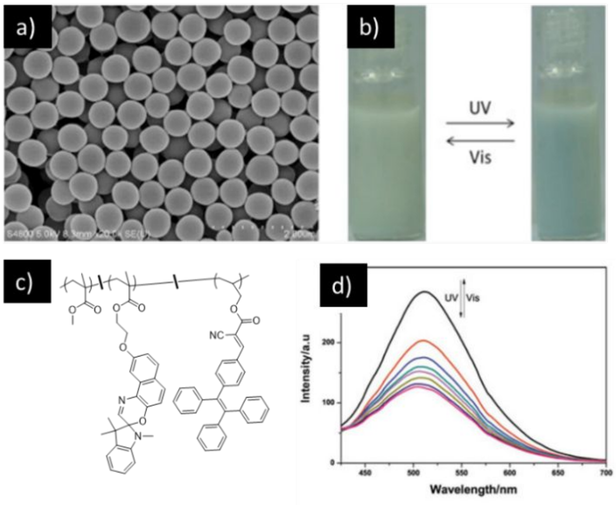

Fig. 11 Li et al. designed latex copolymers containing both AIE luminescent (TPE) and photochromic (SPO) compounds (c) to controllably modulate fluorescence with UV/vis photoswitching (b,d). Copyright 2017. Reproduced with permission from Elsevier from reference 87.

Shown in Fig. 11, Li *et al.* designed polymer particles with both photochromic (via spirooxazine, SPO) and AIE luminescent (via TPE) properties with semi-continuous polymerization.[87] Interestingly, they found an energy transfer between the SPO (acceptor) and TPE (donor) moieties, which modulated the observed fluorescence from the latter. SPO in the merocyanine isomer absorbed (400-700 nm) nearly the same range of wavelengths emitted by the fluorescing TPE (450-600 nm), and therefore net fluorescence of the colloid was controllably and reversibly switched on or off with visible or UV light, respectively.

As a unique strategy to incorporate AIEgens into latex, the Xie group fabricated TPE-grafted silica colloids (sols) in water, which served as seeds for semibatch emulsion polymerization of an acrylic polymer shell around the silica core.[88] As stated previously, AIEgens require restriction of rotation for their fluorescent properties. The authors found that grafting TPE onto the silica particles provided some degree of this requisite mobility restriction. However, the addition of the acrylic shell significantly increased fluorescence even further, which suggests additional restriction of TPE's intramolecular rotations by entrapment between the silica and acrylic layers of the particle.

Recent work by Liang *et al.* provides interesting insight into the advantages of the hydrophobic polymer particle environment on AIEgens.[89,90] As shown in Fig. 12, the authors synthesized latex particles via miniemulsion polymerization containing the water-sensitive AIEgen, 1-methyl-1,2,3,4,5-pentaphenylsilole (MPPS).

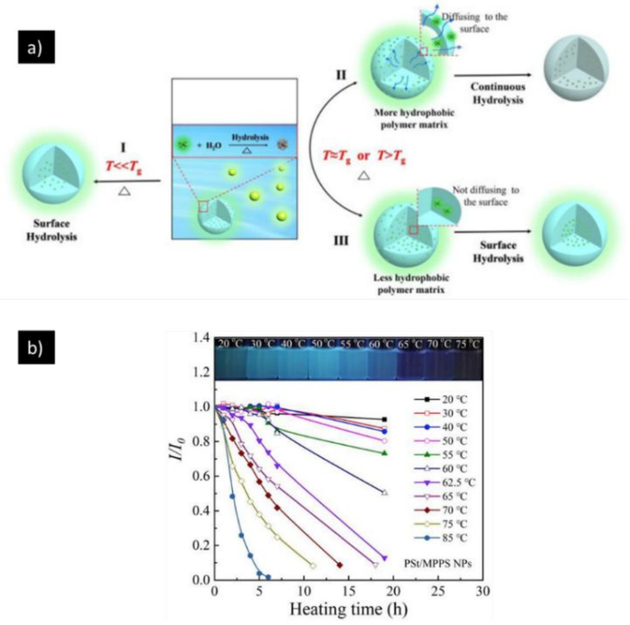

Fig. 12 Liang and coworkers investigated the effects of chain mobility on the protection of water-sensitive AIEgens. (a) Below Tg, AIEgens are kinetically trapped away from the polymer-water interface. However, at and above Tg they can migrate to the surface and hydrolyze. (b) Increased fluorescence loss of MPPS as the temperature approaches the particle Tg (74 °C). Copyright 2019. Reproduced with permission from Elsevier from reference 90.

These particles exhibited temperature-dependent fluorescence loss, attributed to the thermomechanical properties of the polymer. The authors explain that while the hydrophobic interiors of latex particles protect MPPS from hydrolysis, sufficient chain mobility enabled these molecules to migrate to the particle surface where they can be exposed to water and hydrolyze. Decreasing chain mobility through use of glassy polymers like polystyrene improved fluorescence stability by kinetically trapping MPPS units away from the particle surface. At elevated temperatures, above the T_g of the particles, increased mobility removed this protective kinetic barrier evidenced by a loss in fluorescence stability.

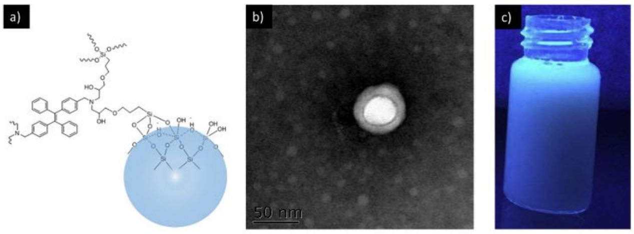

Fig. 13 Li and coworkers designed hybrid latex particles with fluorescent AIE-functionalized silica cores. (a) TPE-modified silica nanoparticle "seed" (b) TEM of core-shell hybrid latex particles (c) fluorescence of hybrid latex. Copyright 2019. Reproduced with permission from Elsevier from reference 88.

Recent work by Li *et al.* introduced AIEgens into latex as TPE-functionalized silica cores.[88] Functionalized silica nanoparticles were prepared via silane coupling of a modified TPE compound onto the surface (Fig. 13). A subsequent emulsion polymerization using these particles as seeds yielded hybrid organic-inorganic latex particles with fluorescent silica cores. Subsequent film formation of the hybrid latexes yielded fluorescent nanocomposite films.

3.2.3. Fluorescence resonance energy transfer (FRET) in latex

Fluorescence resonance energy transfer (FRET) is a phenomenon where an excited donor chromophore molecule transfers energy through dipole-dipole interactions to an acceptor molecule, which causes it to fluoresce.[135] FRET is used throughout chemistry and biology as a light-based probing technique, which involves tracking the unique fluorescence pattern emitted when two species (each tagged with either a FRET donor or acceptor) are within a certain distance of each other.[136,137] Work by Winnik *et al.* utilized FRET as a uniquely powerful tool for fundamental investigations into the interdiffusion of polymer chains between particles during latex coalescence and film formation.[138–143] In the simplest example, their strategy involves the synthesis and mixing of donor- and acceptor-labeled latex particles followed by subsequent film casting under a excitation irradiation to observe FRET fluorescence upon interparticle polymer mixing. Paulis *et al.* provided an interesting use of this approach to investigate the effect of "hairy" layer length on film formation and properties.[144] Asua *et al.* examined the interdiffusion of polymer chains with FRET during the film formation of Pickering dispersions.[145] Rad *et al.* utilizes the photoisomerization of spiropyran (Scheme 1) to provide a photo-switchable FRET acceptor, enabling photo-switchable dual-color fluorescent latex particles.[92,103,110] The authors synthesized latex particles containing both azocarbazole- and spiropyran-functionalized acrylic monomers and observed energy transfer only between the former and the zwitterionic merocyanine isomer of the latter. In the absence of FRET, the azocarbazole moieties fluoresced independently, emitting green visible light. During FRET, the merocyanine isomer fluoresced red. Cerdàn *et al.* investigated FRET within latex particles in the colloidal state and gained unique insight into core-shell particle morphologies through inhomogeneous dye distribution throughout the particle.[146]

3.3 Photothermal and photoacoustic response

Significant research has investigated the unique capabilities afforded by photothermal latex particles, which convert incident light (typically near-infrared (NIR) or green visible light) into heat. These particles are typically synthesized via conventional techniques (e.g. emulsion polymerization) and doped with photothermal agents such as xanthene or cyanine dyes, Fe_3O_4 and gold nanoparticles, or polyaniline.[147] In the colloidal state, transfer of photoinduced heat into the fluid surrounding each particle generates a large, localized thermal gradient and altered refractive index.[148] This phenomenon enables tracking of single particles by monitoring deflections of a "probe" light beam passing near the particle surface.[149] Higher excitation intensities induces dielectric breakdown and plasma formation in the particles, creating extremely high temperatures (10^4 K) in a short amount of time. The resultant explosive expansion generates sound waves and therefore serves as a mechanism for photoacoustic response.[147] Sawada and coworkers introduced a method to utilize this effect to count particles, through measuring acoustic emissions with a piezoelectric sensor, that were otherwise too small to observe through optical techniques.[149–151] Thomas *et al.* used antibody-functionalized, black latex spheres to label breast cancer cells for photoacoustic analysis.[152] The use of an ultrasound detector in place of piezoelectric sensors enabled photoacoustic imaging,[153,154] however the full utilization of polymer latex particles for this technology requires further investigation.

Other approaches take advantage of the photothermal behavior of these particles as a therapy to destroy cancer cells.[155] This typically involves the injection of photothermal agents into a tumor with subsequent irradiation of the tumor. Near-infrared (NIR) and green light have both been investigated as excitation sources due to their ability to penetrate skin and tissue, enabling non-invasive therapies. Asadian-Birjand *et al.* report the use of crosslinked, thermoresponsive "nanogel" (NG) crosslinked polymer particles for this purpose.[156] The authors loaded the NGs with the dye, indocyanine green, to provide photothermal properties. The NG mitigated concerns of poor water solubility, cytotoxicity, and protein binding of the dye without significantly hindering its photoactive effects. The production of singlet oxygen molecules by the dye provided an alternate anti-cancer therapy commonly referred to as "photodynamic" therapy. From the same group, Molina *et al.* introduced semi-interpenetrating polymer network (sIPN) NGs in which the non-crosslinked component was polyaniline, a strong NIR-absorber.[157] The crosslinked network component was poly(N-isopropylacrylamide) (PNIPAM), a well-known thermoresponsive polymer that exhibits a lower critical solution temperature (LCST) (i.e. precipitates/clouds above approximately 32 °C). The NGs showed significant temperature increases ($\Delta T \sim 20$ °C), which enabled selective killing of cells upon NIR irradiation, establishing these particles as promising photothermal therapy agents. Although both examples observed LCST-based shrinkage with photoinduced temperature increases, this phenomenon occurs below average body temperature, and therefore prevented its utilization in *in vivo*. Strong et al. provided an early example of harnessing photothermal shrinkage of NG's for targeted drug delivery.[158] The authors copolymerized NIPAM with acrylamide to increase the LCST from 32 °C to above 40 °C, and they incorporated silica-gold nanoparticles within each NG as photothermal agents. The NG's were subsequently swelled with drugs and remained loaded at physiological temperature (37 °C). In addition to the known benefits of photothermal therapy, NIR triggered drug release upon photothermal shrinkage of these NG's. Chang *et al.* also synthesized modified NIPAM-based NG's with increased LCST.[159] However, this work investigated the use of sodium copper chlorophyllin (SCC) as the photothermal agent, with absorption tuned for green, visible light. Green light is absorbed to a far less extent by water than NIR, allowing for a more targeted energy delivery to the NG's in tissue. As with the previous example, these particles provided simultaneous photothermal therapy and localized drug release. Recent work by Shen and coworkers explored bioinspired PLGA based polymer nanoparticles doped with indocyanine green which also provided photothermal behavior that expedited the release of doxorubicin.[160] Recent work by Ding *et al.* investigated polydopamine as an alternative, bioderived photothermal agent for NG-based photothermal therapy.[161]

As a unique direction for these materials, Shang and coworkers investigated hybrid latexes containing both NIPAM copolymer particles and Fe_3O_4 photothermal nanoparticles for photothermal coatings with switchable underwater oil adhesion.[162] NIR irradiation induced photothermal temperature increases in the film above its LCST, increasing hydrophobicity. This allowed for precise patterning of underwater substrates by the spatially selective NIR irradiation. Xu *et al.* utilized polydopamine as a low-cost photothermal nanoparticle with a facile preparation procedure.[163] The authors added a PNIPAM shell to polydopamine to provide photothermal release of pesticides for agricultural applications.

3.4 Photocatalysis and photo-oxidation in latex

The incorporation of TiO_2 into latex has been heavily investigated throughout paint and coatings industry as well as academia. TiO_2 is primarily used as an opacifier for coatings; however, its strong UV absorbance also introduces highly reactive photochemistry. The well-studied photocatalysis by TiO_2 involves the production of reactive singlet oxygen and hydroxyl radicals from ambient oxygen and water in response to UV irradiation.[164,165] These reactive species react with the polymer matrix, particularly unsaturation in polymer backbones, leading to oxidative degradation of the film. While a large number of efforts seek to reduce this photochemistry to prolong longevity, primarily through modification of the titania surface or crystalline morphology,[166–169] it provides unique opportunities for functional coatings. A major focus utilizes these reactive species to degrade organic compounds and bacteria, providing a photoactivated "self-cleaning" mechanism for latex coatings.[164,165,170–174] Additionally, Martinez *et al* investigated the use of TiO_2-containing films to degrade various nitrogenous oxides (NO_x) from the air through photocatalytic oxidation.[175] The majority of examples mix TiO_2 dispersions into latexes to create hybrid colloids.[176] However, this method is prone to aggregation of the inorganic filler, which reduces surface area and its photocatalytic capability in the film. Miniemulsion and related techniques address this by incorporating TiO_2 nanoparticles within each polymer latex particle,[172,177] however this encapsulation also reduces the availability of the photocatalyst to air which hinders its efficacy. González *et al.* reports the first use of Pickering miniemulsion polymerization to address these issues for photocatalytic TiO_2 latexes.[171] This approach yielded polymer latex particles with titania nanoparticles presented on their surfaces. As a result, these photocatalytic agents were readily accessible at the surface of coalesced films and displayed efficient self-cleaning behavior and E. coli in response to UV irradiation.[178] Interestingly, the TiO_2 nanoparticles at the surface yielded a honey-comb distribution of these fillers in the coalesced film. From the same group, Bonnefond *et al.* provided an interesting advancement of these Pickering dispersions with the addition of magnetite (Fe_3O_4) nanoparticles within the particles in addition to TiO_2 at the surface; this enabled facile recovery and recycling of the multifunctional photocatalytic latex particles. In addition to TiO_2, ZnO has also been investigated as a photocatalytic agent in latex formulations, with promising results of increased photocatalytic performance than TiO_2.[179,180]

3.5 Photomechanical response

The transduction of electromagnetic radiation into mechanical energy enables the unique ability to manipulate polymer particles with light. Mechanochemistry is a rapidly expanding field, providing exciting capabilities to materials that include shape memory, locomotion, and stress-analysis.[181] Photo-activated mechanochemistry primarily utilizes photoisomerization of mechanically active linkages in materials. Specifically, a major portion of research in this area focuses on the photoisomerization of the azobenzene chromophore, shown in Scheme 2. Upon irradiation at approximately 320 nm, the molecule isomerizes to the *cis* form.[182] It is important to note that while one isomer dominates upon irradiation at either wavelength, it is neither quantitative nor static; an equilibrium exists between the two forms at all times. The rapid excitation and relaxation between isomers results in a continuous cycling between the cis and trans states during irradiation.

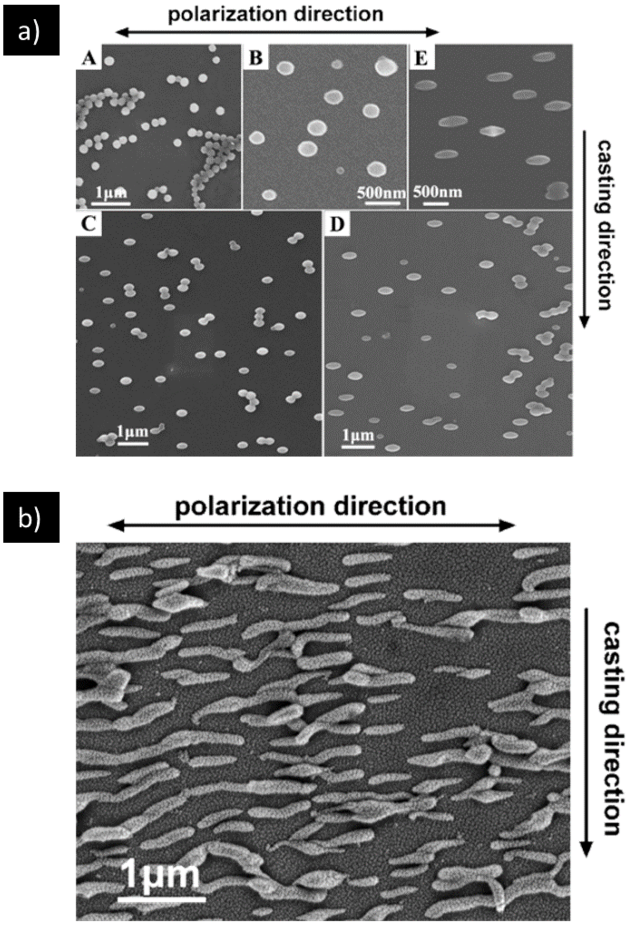

Fig. 14 Li and coworkers investigated the photomechanical deformation of azobenzene containing polymer particles. Irradiation times of 5 (A), 10 (B), 15 (C), 20 (D), and 30 (b) min. Copyright 2006. Reproduced with permission from the American Chemical Society from reference 183.

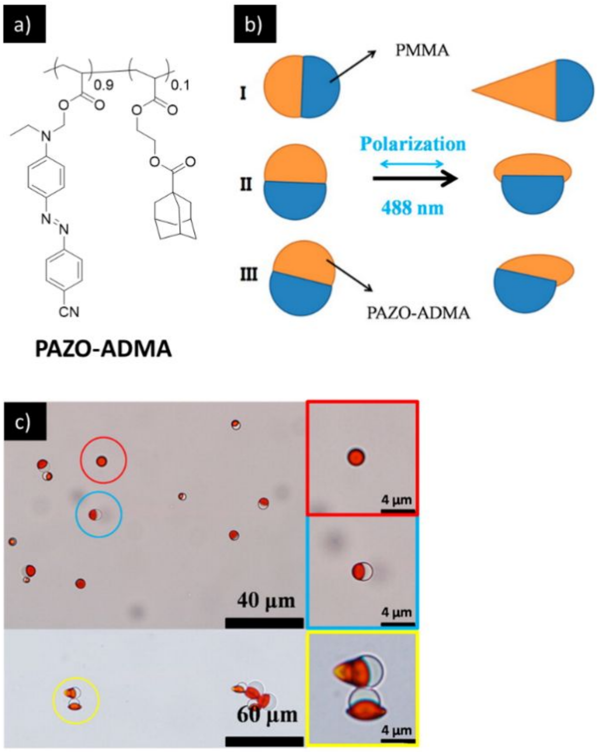

Fig. 15 Zhou and coworkers investigated the photo-deformation of Janus azo-functionalized latex particles. (a) Azo-containing copolymer incorporated into one half of the Janus particles. (b) Effect of orientation on shape of photo-deformed particle (c) optical micrograph of Janus particles before (top) and after (bottom) irradiation. Copyright 2016. Reproduced with permission from the American Chemical Society from reference 189.

Li and coworkers discovered the curious photomechanical deformation of polymer particles, which contained azobenzene units pendant to the polymer chain, shown in Fig. 14.**[183,184]** The authors irradiated the particles with a p-polarized laser, which has an electric field parallel to the plane of incidence, at 480 nm and observed an elongation of the particles along the direction of the light polarization. While the precise mechanism of this response remains unknown, the authors point to similar work which examines the photomechanical effect of azo-functional polymers in the film state. Kumar *et al.* attributed the photo-induced deformation of azo polymers to the trans-cis cycling of the azobenzene units during irradiation.[185] These wagging motions lead to “photo-induced plasticization” and local volume changes of the glassy polymers, resulting in a mechanical pressure between light and dark regions. This “gradient force” therefore provides deformation of azo-functional polymers and may contribute to the deformation observed by Li and coworkers for azo-functional polymer latex particles. Kumar and coworkers attribute an observed reliance of deformation on p- versus s-polarized light on induced polarization effects. Similar observations by Lambeth and coworkers from azo-functional particles formed from ring-opening metathesis polymerization (ROMP) and subsequent emulsification support these findings.[186] Various subsequent studies provide examples of similar effects in many other compositions for both pendant[187–190] and main-chain azo functionalities.[35]

Zhou *et al.* provide an interesting advancement of photo-deformable particles with the introduction of azo-functionalized Janus latex particles.[189] The authors synthesize these via emulsification of a solution containing poly(methyl methacrylate) (PMMA) and the azo-functionalized polymer, PAZO-ADMA, shown in Fig. 15. The two polymers phase-separated after particle formation, yielding Janus polymer nanoparticles. As only one half of the Janus particle is photoresponsive, this system enables the unique ability to study the effect of orientation (with respect to the direction of p-polarization) on the deformation shape. Various shapes occur as the force alignment yields either tension or shearing forces on the PAZO-ADMA side of the sphere. Work by Hsu and coworkers designed “strawberry” Janus polymer particles via the blending of an azo-functional glass with PDMS oligomers.[191]

Shown in Fig. 16, Hou and coworkers investigated Janus polymer particles which contain an azo-functional liquid crystalline (LC) polymer on one side.[192] Upon light-induced cis-trans cycling of the azo-end groups, as discussed earlier, the LC phase becomes amorphous and expands before eventually engulfing the other half of the particle. Visible light reverts the azobenzene groups primarily to the trans state and the particles revert to the Janus morphology.

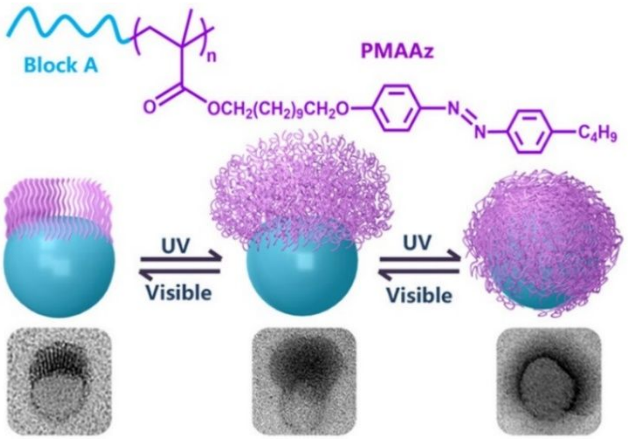

Fig. 16 Hou et al. investigated the synthesis and photoresponse of LC azo-functionalized particles with reversible “self-engulfing” behavior. Copyright 2018. Reproduced with permission from the American Chemical Society from reference 192.

Recent work by Lee and coworkers utilized photocleavable surfactants to adjust the microphase-separated morphology within block copolymer latex particles and elicit a change in shape.[193] In the case of hybrid particles, multiple interfaces exist within a single particle. In addition to an investigation of surfactant-water interactions, this study also probes interactions between the surfactant and each polymer chain within the particle. Upon irradiation of UV light, the hydrophobic tails of the designed surfactants detached, while the hydrophilic, water-facing head remained unchanged. As a result, the particles remained stable in water while the relative affinity of each polymer with the surfactant changed dramatically. Cleavage of this hydrophobic tail reduced its affinity for polystyrene (in a PS-*b*-P2VP block copolymer) and increased its affinity for the poly(2-vinylpyridine) (P2VP) block. Shown in Fig. 17, this evoked a rearrangement of the block microphase separation within the particle from an “onion-like” core-shell morphology (where only PS interacted with the surfactant) to a stacked lamellar morphology (where P2VP interacted with the cleaved fraction of surfactant molecules). This latter morphology necessitated a change in overall particle shape to permit each block access to the surfactant. At high degrees of surfactant photocleavage, the onion-like morphology returned as the inverse case, with predominantly P2VP at the surface.

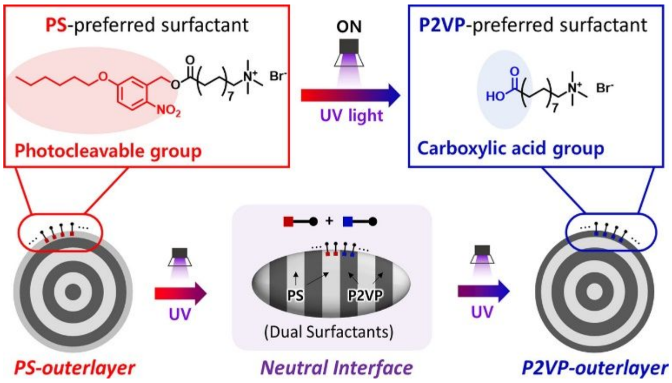

Fig. 17 Lee and coworkers investigated the use of photocleavable surfactants to yield changes in block microphase-separated morphology within latex particles and, as a result, the overall particle shape. Copyright 2019. Reproduced with permission from the American Chemical Society from reference 193.

3.6 Photo-induced particle aggregation

The controlled disruption of colloidal stability in latex remains a leading focus in latex research and provides versatility for isolating polymer particles and/or solidifying a liquid latex by more efficient means than drying and film formation. Investigations encompass a variety of stimuli including solvent dilution and centrifugation,[194] pH,[61,195,196] temperature,[197] salt/flocculant addition,[198] polymer bridging,[199] shear,[200] and gas exposure.[201] Light provides a rapid, low cost, selective, and controllable stimulus, and therefore an ideal trigger for the controlled aggregation of latex colloids.

The colloidal stability of latex particles in water relies on their Brownian motion and repulsion from other particles.[202–204] At submicron sizes, the stochastic movement of these particles dominates the gravitational force which would otherwise cause them to sediment. Therefore, an increase in size due to particle aggregation slows this motion and disrupts colloidal stability. Free or covalently bound surfactant molecules prevent this by providing charge at the particle surface. Surface charges induce repulsion between particles due to van der Waals and double layer forces as described by DLVO theory.[202–204] The surfactant’s critical role in colloidal stability highlights this component as the target of most triggered aggregation mechanisms, including via photochemical pathways.

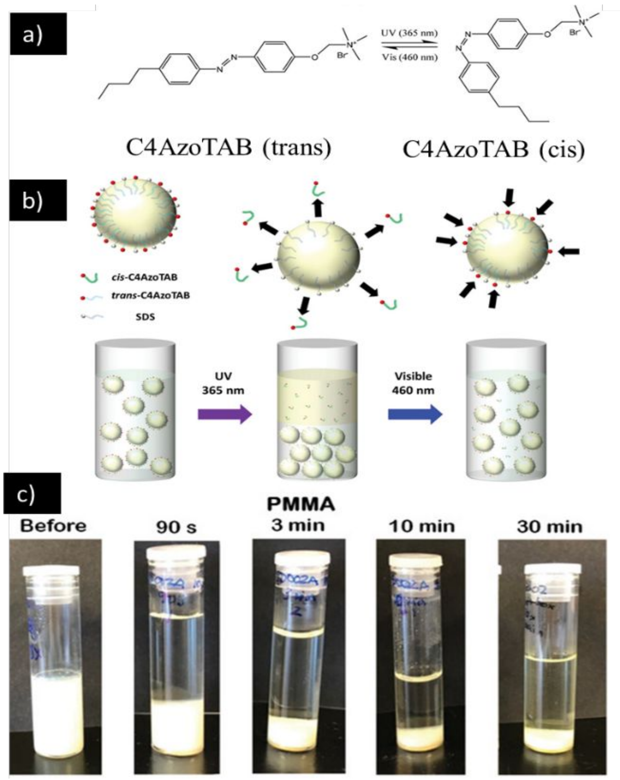

Fig. 18 Jasinski et al. introduced the ability photo-induce aggregation of latex via incorporation of an azo-functionalized photosurfactant. Copyright 2019. Reproduced with permission from John Wiley & Sons, Inc from reference 209.

Photoresponsive surfactants, or photosurfactants, enable photolabile colloidal stability.[205–207] These unique molecules disrupt or reinforce their stabilizing capabilities by changing shape via cis-trans isomerization, losing/altering amphiphilicity via photoscission, changing head group polarity via chemical transformations, or coupling through polymerization or dimerization.[205] While the majority of photosurfactant studies are limited to small molecule colloids[208], the burgeoning investigation of these molecules for latex shows promise for a new avenue for triggered particle aggregation.

Recent work by Jasinski *et al.* provides a leading example of the promise for photosurfactants in latex.[209] As described previously for photomechanical applications, azobenzene isomerizes to either predominately cis or trans in response to UV or visible irradiation. Within a surfactant, this isomerization dramatically affects how the molecule interacts with the polymer-water interface by changing the overall polarity of the molecule. Shown in Fig. 18, the authors suggest that upon UV irradiation, the azo-functional surfactant,C4AzoTab, isomerizes to the cis form which is more water-soluble (higher critical micelle concentration, CMC) and therefore desorbs from the particle surface to dissolve into the aqueous phase. As the surface becomes increasingly bare, the colloidal stability diminishes and the particles aggregate. However, this process is reversible. Upon visible light irradiation, the surfactant returns to predominantly the *trans* isomer and reinserts into the particle surface, enabling particle redispersion. The inclusion of a non-photosensitive and oppositely charged surfactant, sodium dodecyl sulfate (SDS), facilitates both aggregation and redispersion. SDS provides a low level of negative charge at the surface which aids the overall decrease in zeta potential as the positively charged C4AzoTAB leaves the surface. This charge also provides enough repulsion in the aggregated state to prevent irreversible coagulation.

In addition to photosurfactants, aggregation is induced by the introduction of attractive interactions on the particle surface. In this way, spiropyran-functionalized latex particles developed by Abdollahi *et al.* (described previously in this review for their photochromic properties) exhibit photoinduced aggregation for particles containing sufficient concentrations of SP on their surfaces.[107] Illustrated in Fig. 19, the authors designed latex with varying amounts of SP on the surface and observed significant size increases after UV irradiation, with the greatest size increases corresponding with the highest SP loadings. The authors explain that upon formation of the zwitterionic merocyanine (MC) form, electrostatic and π-π interactions provide attractive interactions

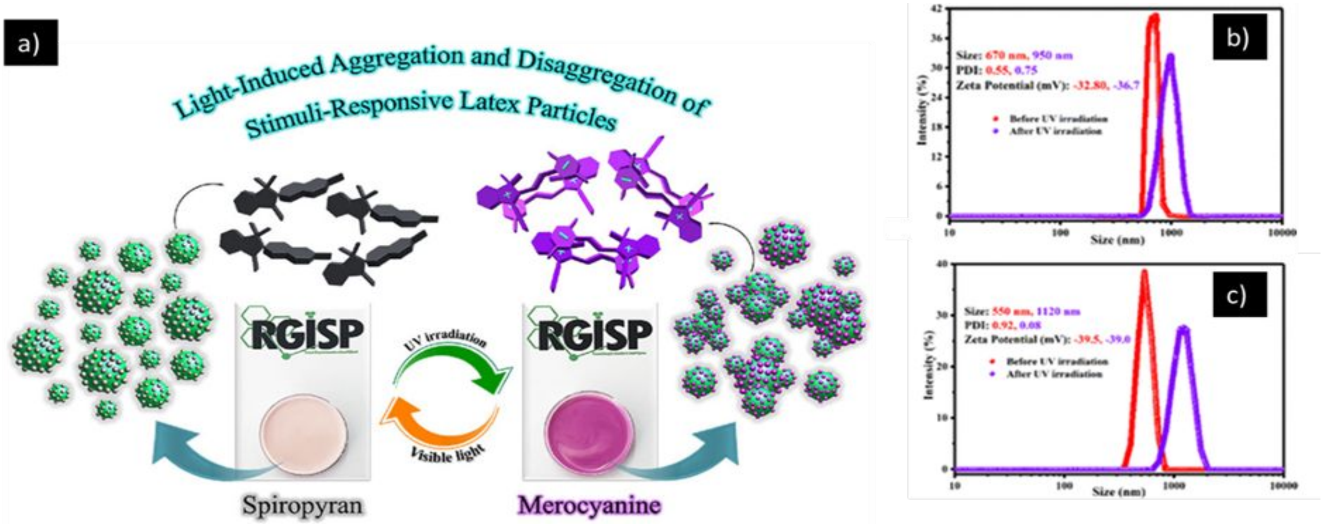

Fig. 19 Abdollahi *et al.* investigated the (a) reversible photo-induced aggregation of spiropyran (SP) surface-functionalized latex particles. DLS showed size increases at concentrations from 0.5% (b) to 5% SP (c). Copyright 2018. Reproduced with permission from the American Chemical Society from reference 107.

without significantly affecting the overall zeta potential of the particles. The presence of this charge (provided by the SDS in the previous example) enables redispersion of the particles upon photo-reversal of the MC functional group under visible light.

The inclusion of coumarins in polymers enables a range of photo-functionality including light harvesting and photocrosslinking.[32,34] Chung *et al.* provides a unique approach to photoaggregation of latex particles via coumarin cycloaddition photochemistry.[33] The authors fabricate latex particles from homotelechelic coumarin end-capped poly(ε-caprolactone) oligomers via flash nanoprecipitation. The authors report size increase of the particles in response to UV (365 nm) due to coumarin dimerization between particles. Analogous to previous examples, this dimerization is photoreversible at lower wavelengths (254 nm), which enables redispersion of the aggregated particles. However, the size change reported by the authors is minor compared to other examples, evident by the appearance of a minor, higher diameter tail on the DLS size distribution. This may be due to the slow kinetics of coumarin dimerization, and the lack of forced localization of these moieties at the surface, as accomplished in other examples via seeded semibatch emulsion polymerization or the use of reactive surfactants. Yuan *et al.* provides another example of using coumarin chemistry to photochemically cluster silane-based particles.[210]

3.7 Interparticle photocrosslinking

Crosslinking and network formation represent a heavily studied research focus for both photochemistry and latex, primarily to increase the mechanical properties and chemical resistance of the resultant polymer film. Photocrosslinking in latex has occurred primarily as intraparticle photocrosslinking in the colloidal state (discussed previously), film-state photocrosslinking between chains from every particle after drying and coalescence of the latex, and colloidal state interparticle photocrosslinking to connect the dispersed latex particles and yield a solid. The latter in particular affords exciting new opportunities beyond traditional film and coatings applications.

3.7.1 Film-state photocrosslinking Latex design to yield photocrosslinkable coatings and films has received major attention across both academia and industry. As mentioned previously (Fig. 1), Schlögl *et al.* introduced photocrosslinking chemistry into natural latex capable of crosslinking the polydiene backbone in either the latex state (intraparticle crosslinking) or after drying into the film state to yield a macroscopic crosslinked network.[24] This light driven alternative to traditional vulcanization chemistry provides significant advantages to traditional approaches; a crosslinked network of high molecular weight polymer can be fabricated without energy intensive high-shear mixing and heating or the use of toxic inorganic sulfur compounds.[211,212]

Incorporation of film-state photocrosslinkability also provides major advantages for the paint and coatings industry.[213–217] The resultant films after drying and coalescence of conventional latex are only physically entangled. Because the T_g's of many latex coatings are low to promote film formation (low minimum film-forming temperatures, MFFT), the mechanical properties and chemical resistance of the entangled films are often poor. Crosslinking chemistry addresses this problem by chemically connecting the chains after entanglement to form a robust network. Many paint and coating applications target substrates that undergo exposure to sunlight and UV, and therefore photocrosslinking chemistry exploits this readily available energy source to strengthen the film. Alkyd resins represent one of the most studied crosslinkable latex formulations, which is widely used in the paint industry.[218–221] This process involves oxidative crosslinking, which involves hydrogen abstraction of the allylic hydrogens adjacent to residual double bonds in unsaturated fatty acid substituents. Photosensitizers, such as the dye Rose Bengal or radical photoinitiators, assist this process and decrease the time required to generate a crosslinked film.[218]

Other photocrosslinkable moieties for photocurable latex coatings typically include acrylate and methacrylates[213] which are covalently or ionically incorporated into the polymer backbone. Typical backbones include polyurethanes[215,222–225], polyacrylics[109,214,226], or polydienes (which natively contain crosslinkable alkenes)[25,26,31]. Chen and coworker incorporated latent photocrosslinkability into latex via the design of novel divinyl monomers, which contain alkenes of different reactivity.[227] One alkene readily polymerized into the polymer backbone via radical mechanisms during traditional emulsion polymerization, while the other remained unreacted, yielding a pendant crosslinkable group. Photoinitiator and electron-donating co-monomers were added, the latex mixture was dried into a film, and the film was subsequently irradiated with UV light to initiate photocrosslinking. This approach to the synthesis of crosslinkable polymers via unsaturated repeat units is not dissimilar from diene (butadiene, isoprene, EPDM, etc.) polymerization in which a nonpolymerizable, yet crosslinkable, alkene exists in the repeat units.

Work by the Kawahara group investigated the grafting of photopolymerizable monomers onto latex surfaces to create a crosslinkable "matrix" between the particles after drying and UV exposure.[228,229] To prevent crosslinking of the difunctional molecule, the authors inactivated one of the ends of a diacrylate molecule via cyclodextrin (CD) complexation. The remaining acrylate then reacted with the repeat unit double bonds of natural latex particles, generating polyisoprene particles with grafted acrylate-CD complexes on their surfaces. Thorough washing removed the CD complex, rendering the surface-grafted acrylates bare and labile for photoinitated radical crosslinking.

Recent investigations into thiol-ene[20,21] and thiol-Michael[109] click reactions as step-growth polymerization chemistries in miniemulsion conditions provide promising results for the synthesis of functional latexes. Because the alkenes do not homopolymerize in these conditions, they remain as latent crosslinking sites when polymerized in stoichiometric excess.

Recently, Badía *et al.* synthesized a novel, bio-based and photo-functional monomer, piperonyl acrylate, monomer to provide film photocrosslinking in a sustainable approach.[230] Copolymerization with this monomer via emulsion polymerization yielded piperonyl functionalized latexes. UV exposure after drying and film formation generated radicals via photolysis of these units which enabled photocrosslinking of the film and optimization of film strength and adhesive properties.

3.7.2 Colloid-state interparticle photocrosslinking and attachment

Interparticle photocrosslinking in the colloidal state, which results in the rapid immobilization of particles, remains a burgeoning and vastly promising direction for the future of light and latex. As one form of immobilization, precise photoinitated attachment of particles to substrates creates a novel fabrication strategy for the formation of nanostructured surfaces, which are useful for optical applications.[231–233] In another direction, interparticle crosslinking enables photoactivated liquid-solid transformations of liquid colloids, a highly useful response for a variety of modern technologies, in particular additive manufacturing.[234] Colloidal particles are small, discrete, repulsive, and rapidly moving throughout the continuous phase. Recent work, described previously, investigated methods for attachment between particles to promote aggregation in response to a light stimulus. However, all these examples produce larger particles clusters, not anchored particles or macroscopic solids. While some techniques rely on surface functionalization,[235] other strategies explore the addition of reactive molecules to the continuous phase to generate a network between particles.[233,236,237] Most surface-based techniques rely on aggregation/assembly techniques to bring particles together before immobilization and coupling; as a major advantage, continuous-phase photoreactivity approaches circumvent that requirement.

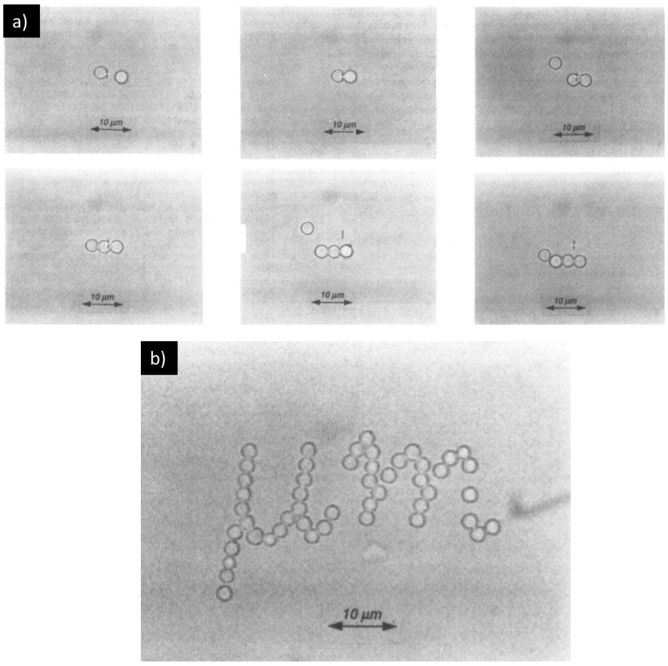

Fig. 20. Misawa *et al.* utilized light to manipulate and photochemically fixate latex particles via laser trapping and continuous-phase photocrosslinking, respectively. (a) This process enables the forced and permanent assembly of latex particles. (b) illustrates the excellent spatial control for this assembly process to enable fabrication of microscopic patterns. Copyright 1993. Modified and reproduced with permission from the American Chemical Society from reference 236.

Misawa and coworkers investigated the use of light to photochemically assemble latex particles, but also to precisely manipulate them in three dimensions, thus forcing them into contact with each other or a substrate beforehand.[236] The authors utilized "laser trapping", a procedure which harnesses the momentum change of light as it is refracted by a particle to exert a precise force that is controllable in three dimensions. The incorporation of the water-soluble monomer (acrylamide, AM), crosslinker (N,N'-methylene-bisacrylamide, MBA), and radical photoinitiator ((4-benzoylbenzyl)-triethylammonium bromide, BBA) enabled the photo-activated network formation in the continuous, aqueous phase around and between the inert polystyrene latex particles. Trapping lasers (λ = 1064 nm) moved particles into intimate contact without polymerizing the reactive species in the continuous phase. Once in contact, a photopolymerization laser (λ = 355 nm) excited the BBA initiator to produce radicals and initiate gel formation precisely at the laser focal point, which was directed at the contact area of the two spheres. Shown in Fig. 20. , subsequent iterations of this process (using one trapping laser to immobilize the growing particle complex) enabled the robust and irreversible assembly of multiple particles with spatial and temporal control. Later work by the same research group investigated this system to attach particles and particle assemblies to a glass substrate.[238]

Marksteiner *et al.* investigated the photochemical "gluing" of polystyrene latex particles together by incorporating monomer into the particles, rather than the continuous phase.[239] The authors prepared crosslinked polystyrene latex particles and subsequently swelled them in additional, unreacted styrene. Due to the lack of reactivity between particles, this approach required aggregation prior to polymerization of the styrene monomer. The authors added salt to screen the electrostatic interactions between particles, which disrupted colloidal stability and induced aggregation. Subsequent UV irradiation polymerized the styrene monomer throughout the particle aggregate, providing particle-particle attachment. This method provides a generalizable strategy; however, it lacks the spatial control of the previous example.

Work by Benkoski *et al.* immobilized particles in a similar fashion to Misawa *et al.*, photopolymerization of crosslinkers between particles, however the novel aggregation method prior to photocrosslinking enabled exciting insight into colloidal interactions. Shown in Fig. 21, the authors coated a glass slide with the

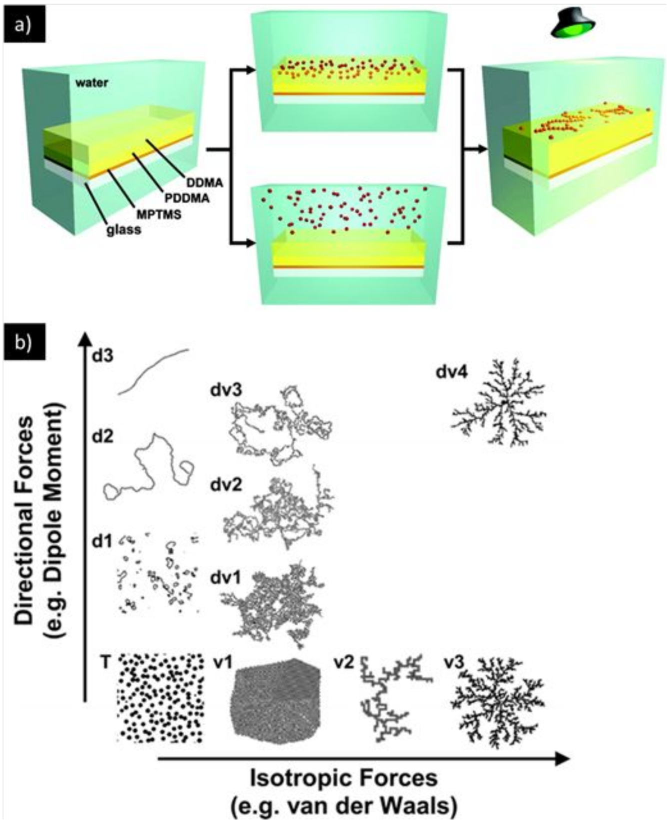

Fig. 21 (a) Platform developed by Benkoski *et al.* enabling the photo-initiated immobilization of latex particles assembled at an oil-water interface. (b) This platform enables investigation of the interplay of forces between colloidal particles and their effect on aggregation morphology. Copyright 2007. Modified and reproduced with permission from the American Chemical Society from reference 237.

crosslinkable monomer, 1,12-dodecanediol dimethacrylate (DDMA), and dipped it into water, forming an oil-water interface. Latex particles, dispersed in either phase, migrate to the interface and aggregate there. Photocrosslinking of the oil phase locked the interface into a solidified "fossil". Subsequent imaging of these interfaces enabled unique access to study the interactions and aggregation behavior for various types of colloidal particles.

3.7.3 Light and latex for additive manufacturing Vat photopolymerization (VP) additive manufacturing, otherwise termed stereolithography, is a 3D printing platform that fabricates objects with light at a resolution and geometric complexity beyond most other manufacturing techniques.[234] This process generates three-dimensional objects in a layer-by-layer approach through iteratively photocuring layer "slices" at the surface of liquid photopolymer resin with UV or visible light. Each photocured layer is dipped below the surface and recoated with liquid resin before repeating the process to create the next layer. As such, photopolymer materials must rapidly undergo a rapid and spatially selective liquid-to-solid transition in response to light exposure. Photocuring chemistry typically relies on rapid, well-studied crosslinking chemistry such as multi-functional acrylate polymerization[240–244] and thiol-ene click reactions[245,246]. Zhu *et al.* provided an excellent review of colloidal materials for 3D printing, many of which for VP are ceramic suspensions and small molecule emulsions.[247] Despite their molecular weight, polymer colloids naturally exhibit low viscosities which are ideal for this process; however, their adoption as VP printable materials demands major innovation in latex photochemistry.

The Doyle group investigated the unique heat-induced aggregation, "thermogelling", of polymer colloids with subsequent photocrosslinking to irreversibly secure the particles together.[59,248] The authors introduced the water-soluble, oligomeric crosslinker, poly(ethylene glycol) diacrylate (PEGDA), to colloidal poly(dimethyl

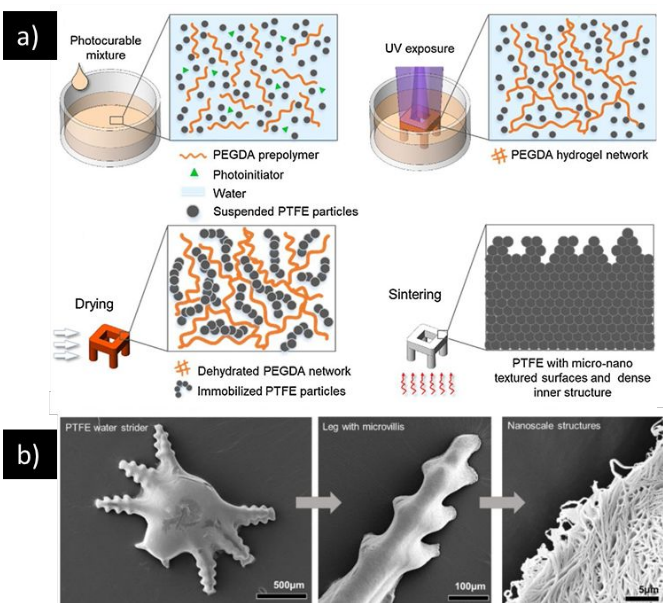

Fig. 22 3D printing of thermo- and photo- responsive PDMS colloids by Doyle *et al*. Copyright 2017. Reproduced from reference 11 via Creative Commons License (CC BY-NC 3.0). Published by the Royal Society of Chemistry.

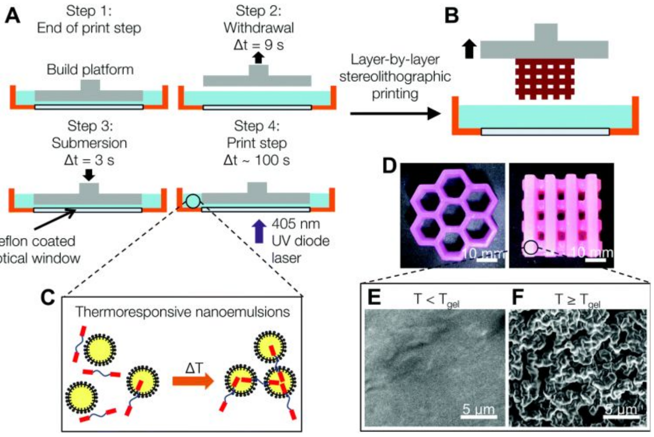

Fig. 23 (a) Zhang et al. printed PTFE colloids via continuous-phase photocrosslinking followed by subsequent thermal degradation of the PEGDA scaffold and sintering of the PTFE particles. (b) 3D printed bionic insect mimics represent an intriguing application for this novel processing capability for PTFE. Copyright 2018. Reproduced with permission from Elsevier from reference 249.

siloxane) (PDMS). Upon heating above a critical gelation temperature, T_{gel}, the liquid colloid solidifies. The authors suggest that this may be caused by insertion of the PEGDA into multiple particle interfaces, effectively bridging particles into a solid, physical network. This thermal gelation effect proved reversible; however, UV-induced radicals (via a photoinitiator) polymerized the PEGDA in the bridged state, permanently securing the solid network where irradiated. The Doyle group introduced this system as an early example of the VP printing of polymer colloids, an exciting new application beyond the traditional 2D applications of latex.[11] Using a modified printer, the authors printed both below and above T_{gel} to generate hydrogels with either discrete PDMS particles or bridged PDMS phases. Subsequent toluene extraction of the PDMS yielded crosslinked PEGDA hydrogels with either continuous or discrete porosity.

Shown in Fig. 23, Zhang and coworkers investigated 3D printing colloids by a similar continuous-phase photocrosslinking approach, however with removal of the photocured network rather than polymer particles after printing. [12,249] Their selection of a PTFE latex provided significant thermal stability of the polymer particles over the photocured “scaffold” that immobilized them into a 3D structure. Thermal treatment degraded the crosslinked PEGDA and sintered the PTFE particles without loss of macroscopic part resolution. This enabled the additive manufacturing of a polymer with challenging processing requirements to yield complex, porous PTFE architectures with micron scale resolution. 3M has developed a commercial process similar to this approach for VP printing of PTFE particles.[250–252]

Recent work in our group by Scott and Meenakshisundaram *et al.* designed a versatile approach to utilize photocurable latex to introduce high molecular weight polymers, and their mechanical properties, to VP additive manufacturing.[10] Illustrated in Fig. 24, a continuous-phase photocrosslinkable network enabled the requisite light-activated, liquid-solid transition to fabricate 3D architectures. After printing, the 3D “green body” consisted of a photocrosslinked hydrogel embedded with latex particles. Thermal post-processing removed water and enabled the latex particles to coalesce *throughout* the scaffold, yielding a semi-interpenetrating polymer network (sIPN). This novel approach to sIPN formation removes the requirement for high thermal stability as it allows particle coalescence without thermal degradation of the scaffold. Shrinkage occurs isotopically and neither it nor the network penetration by the latex polymers disrupt the printed features shape and resolution. This work also introduces in-situ computer-vision print parameter optimization to mitigate light scattering by the colloids and improve feature resolution of printed parts. As a result, this work combines the low viscosity processing advantages of polymer latex, the enhanced mechanical properties associated with high molecular weight polymer, and the ability to fabricate structures with unprecedented spatial and temporal control afforded by photochemistry.

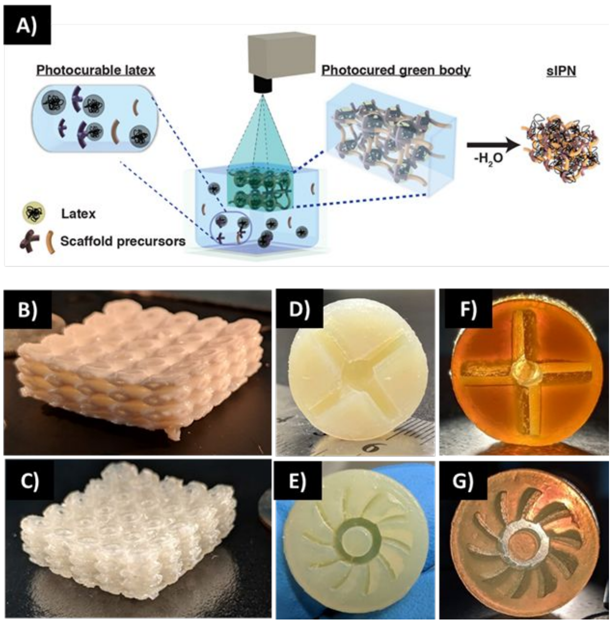

Fig. 24 Scott and Meenakshisundaram *et al.* designed (A) a platform to harness photocurable latex for introducing high molecular weight polymers to VP 3D printing. Images of 3D printed lattice in greenbody (B) and IPN (C). Elastomeric molds (D-G) exhibit combination of geometric complexity and elastic performance. Copyright 2020. Reproduced with permission from the American Chemical Society from reference 10.

4. Future Perspectives for the Role of Light in Latex

Photochemistry revolutionizes traditional strategies for the manufacturing, modification, and manipulation of polymer latexes, introducing new possibilities of these historic colloids as functional nanomaterials. Significant research elucidates colloidal particles as ideal nanostructures for assembly into photonic crystals,[231,232,253,254] enabling optical applications in laser[232] and lens[255] technology. For these applications, particles are typically concentrated and dried onto a substrate to promote self-assembly into colloidal crystal structures. However, previously discussed developments in particle laser trapping and attachment could significantly impact this technology by allowing precise and intentional arrangement of particles for more intricate optical devices. In a similar direction, Tian and coworkers provides an intriguing example of interparticle crosslinking to provide tough photonic crystals.[233] Recent work by Klinger and coworkers introduces photo-degradable crosslinked polymer particles[256,257] which have clear application for triggered drug delivery among other applications. Extensive research into semibatch and ab-initio emulsion polymerization techniques demonstrates uniquely precise control of latex particles over a wide range of sizes.[19,258,259] This combined with synthetic control of surface functionality, modulus, chemical composition, and shape, positions degradable latex particles as promising nanodevices for selective functionality within biological systems. Recent examples of 3D printing latex demonstrate its ability to create crosslinked structures with controlled nanoporosity or fabricate complex architectures of polymer compositions and molecular weights otherwise difficult or impossible to achieve by traditional techniques. The introduction of hybrid colloids to this strategy suggests facile access to nanocomposite materials as a natural advancement of their traditional use in coatings and films. Further, this technology offers potential disruption to fields outside of science and engineering.

Decades of research into the controlled coloration of latexes enables an immense variety of water-based paints. Now, with the ability to 3D print structures from latex, multi-material additive manufacturing, and the current availability of 3D design software, artistic painting ventures can now be reimagined in three dimensions.

Conflicts of interest

There are no conflicts of interest to declare.

Acknowledgements

The authors acknowledge the National Science Foundation for financial support (CMMI-1762712).

References

1 J. M. Asua, *Polymeric Dispersions: Principles and applications*, Springer-Science+Business Media, B.V., Dordrecht, 1997.

2 Emulsion Polymers Market Size, Share & Trends Analysis Report By Product (Acrylic, Styrene Butadiene Latex, Vinyl Acetate Polymers), By Application (Paints & Coatings, Adhesives), And Segment Forecasts, 2019 - 2025, https://www.grandviewresearch.com/industry-analysis/emulsion-polymer-market.

3 Synthetic Latex Polymers Market - Forecasts from 2019 to 2024, https://www.researchandmarkets.com/research/c2lwkn/synthetic_latex?w=12.

4 J. M. Asua, *J. Polym. Sci. Part A Polym. Chem.*, 2004, **42**, 1025–1041.

5 K. Li and B. Liu, *Chem. Soc. Rev.*, 2014, **43**, 6570–6597.

6 C. Pichot, *Curr. Opin. Colloid Interface Sci.*, 2004, **9**, 213–221.

7 V. Kozlovskaya, B. Xue and E. Kharlampieva, *Macromolecules*, 2016, **49**, 8373–8386.

8 B. Sun, Z. He, Q. Hou, Z. Liu, R. Cha and Y. Ni, *Carbohydr. Polym.*, 2013, **95**, 598–605.

9 M. H. Sharifian, A. R. Mahdavian and H. Salehi-Mobarakeh, *Langmuir*, 2017, **33**, 8023–8031.

10 P. J. Scott, V. Meenakshisundaram, M. Hegde, C. Kasprzak, C. Winkler, K. Feller, C. B. Williams and T. E. Long, *ACS Appl. Mater. Interfaces*, , DOI:10.1021/acsami.9b19986.

11 L. C. Hsiao, A. Z. M. Badruddoza, L.-C. Cheng and P. S. Doyle, *Soft Matter*, 2017, **13**, 921–929.

12 Y. Zhang, M. Yin, O. Xia, A. P. Zhang and H. Tam, in *2018 IEEE Micro Electro Mechanical Systems (MEMS)*, 2018, pp. 37–40.

13 H. G. Yuan, G. Kalfas and W. H. Ray, *J. Macromol. Sci. Part C*, 1991, **31**, 215–299.

14 S. Kawaguchi and K. Ito, ed. M. Okubo, Springer Berlin Heidelberg, Berlin, Heidelberg, 2005, pp. 299–328.

15 R. Arshady, *Colloid Polym. Sci.*, 1992, **270**, 717–732.

16 O. Thioune, H. Fessi, J. P. Devissaguet and F. Puisieux, *Int. J. Pharm.*, 1997, **146**, 233–238.

17 G. Akay and L. Tong, *J. Colloid Interface Sci.*, 2001, **239**, 342–357.

18 F. Jasinski, P. B. Zetterlund, A. M. Braun and A. Chemtob, *Prog. Polym. Sci.*, 2018, **84**, 47–88.

19 F. Jasinski, E. Lobry, L. Lefevre, A. Chemtob, C. Croutxe-Barghorn, X. Allonas and A. Criqui, *J. Polym. Sci. Part A Polym. Chem.*, 2014, **52**, 1843–1853.

20 F. Jasinski, A. Rannée, J. Schweitzer, D. Fischer, E. Lobry, C. Croutxé-Barghorn, M. Schmutz, D. Le Nouen, A. Criqui and A. Chemtob, *Macromolecules*, 2016, **49**, 1143–1153.

21 F. Jasinski, E. Lobry, B. Tarablsi, A. Chemtob, C. Croutxé-Barghorn, D. Le Nouen and A. Criqui, *ACS Macro Lett.*, 2014, **3**, 958–962.

22 F. Jasinski, E. Lobry, A. Chemtob, C. Croutxe-Barghorn, L. Vidal, L. Josien, J. Brendlé and A. Criqui, *Colloid Polym. Sci.*, 2014, **292**, 3095–3102.

23 C. E. Hoyle and C. N. Bowman, *Angew. Chemie Int. Ed.*, 2010, **49**, 1540–1573.

24 S. Schlögl, M.-L. Trutschel, W. Chassé, I. Letofsky-Papst, R. Schaller, A. Holzner, G. Riess, W. Kern and K. Saalwächter, *Polymer (Guildf).*, 2014, **55**, 5584–5595.

25 S. Schlögl, A. Temel, R. Schaller, A. Holzner and W. Kern, *Rubber Chem. Technol.*, 2010, **83**, 133–148.

26 S. Schlögl, A. Temel, R. Schaller, A. Holzner and W. Kern, *J. Appl. Polym. Sci.*, 2012, **124**, 3478–3486.

27 J. K. G. Dhont, *Phys. A Stat. Mech. its Appl.*, 1983, **120**, 238–262.

28 C. F. Bohren and D. R. Huffman, *Absorption and Scattering of Light by Small Particles*, John Wiley & Sons Inc., 1983.

29 D. Lenko, S. Schlögl, A. Temel, R. Schaller, A. Holzner and W. Kern, *J. Appl. Polym. Sci.*, 2013, **129**, 2735–2743.

30 N. Hansupalak, S. Srisuk, P. Wiroonpochit and Y. Chisti, *Ind. Eng. Chem. Res.*, 2016, **55**, 3974–3981.

31 P. Wiroonpochit, K. Uttra, K. Jantawatchai, N. Hansupalak and Y. Chisti, *Ind. Eng. Chem. Res.*, , DOI:10.1021/acs.iecr.7b01133.

32 S. R. Trenor, A. R. Shultz, B. J. Love and T. E. Long, *Chem. Rev.*, 2004, **104**, 3059–3078.

33 J. W. Chung, K. Lee, C. Neikirk, C. M. Nelson and R. D. Priestley, *Small*, 2012, **8**, 1693–1700.

34 R. H. Huyck, S. R. Trenor, B. J. Love and T. E. Long, *J. Macromol. Sci. Part A*, 2007, **45**, 9–15.

35 B. Tang, Y. Zhou, Z. Xiong and X. Wang, *RSC Adv.*, 2016, **6**, 64203–64207.

36 P. Gupta, S. R. Trenor, T. E. Long and G. L. Wilkes,

Macromolecules, 2004, **37**, 9211–9218.

37 D. Shi, M. Matsusaki, T. Kaneko and M. Akashi, *Macromolecules*, 2008, **41**, 8167–8172.

38 M. Albuszis, P. J. Roth, W. Pauer and H.-U. Moritz, *Polym. Chem.*, 2016, **7**, 5414–5425.

39 J. Li, L. Wang and B. C. Benicewicz, *Langmuir*, 2013, **29**, 11547–11553.

40 M. J. Penelas, G. J. A. A. Soler-Illia, V. Levi, A. V Bordoni and A. Wolosiuk, *Colloids Surfaces A Physicochem. Eng. Asp.*, 2019, **562**, 61–70.

41 E. Passaglia, S. Coiai and S. Augier, *Prog. Polym. Sci.*, 2009, **34**, 911–947.

42 F. Romani, E. Passaglia, M. Aglietto and G. Ruggeri, *Macromol. Chem. Phys.*, 1999, **200**, 524–530.

43 F. Ciardelli, M. Aglietto, M. B. Coltelli, E. Passaglia, G. Ruggeri and S. Coiai, in *Modification and Blending of Synthetic and Natural Macromolecules*, eds. F. Ciardelli and S. Penczek, Springer Netherlands, Dordrecht, 2004, pp. 47–71.

44 M. Semsarilar, V. Ladmiral and S. Perrier, *Macromolecules*, 2010, **43**, 1438–1443.

45 M. Ballauff, *Macromol. Chem. Phys.*, 2003, **204**, 220–234.

46 X. Guo, A. Weiss and M. Ballauff, *Macromolecules*, 1999, **32**, 6043–6046.

47 S. Tsuji and H. Kawaguchi, *Langmuir*, 2004, **20**, 2449–2455.

48 S. L. Canning, G. N. Smith and S. P. Armes, *Macromolecules*, 2016, **49**, 1985–2001.

49 B. Charleux, G. Delaittre, J. Rieger and F. D'Agosto, *Macromolecules*, 2012, **45**, 6753–6765.

50 J. Tan, H. Sun, M. Yu, B. S. Sumerlin and L. Zhang, *ACS Macro Lett.*, 2015, **4**, 1249–1253.

51 K. Ren and J. Perez-Mercader, *Polym. Chem.*, 2017, **8**, 3548–3552.

52 B. Couturaud, P. G. Georgiou, S. Varlas, J. R. Jones, M. C. Arno, J. C. Foster and R. K. O'Reilly, *Macromol. Rapid Commun.*, 2019, **40**, 1800460.

53 S. C. Thickett and G. H. Teo, *Polym. Chem.*, 2019, **10**, 2906–2924.

54 J. Yeow, O. R. Sugita and C. Boyer, *ACS Macro Lett.*, 2016, **5**, 558–564.

55 L. Yang, J. Xu, J. Han, Y. Shen and Y. Luo, *Ind. Eng. Chem. Res.*, 2015, **54**, 5536–5542.

56 Y. Huang, J. Yuan, J. Tang, J. Yang and Z. Zeng, *Eur. Polym. J.*, 2019, **110**, 22–30.

57 L. Delafresnaye, N. Zaquen, R. P. Kuchel, J. P. Blinco, P. B. Zetterlund and C. Barner-Kowollik, *Adv. Funct. Mater.*, 2018, **28**, 1800342.

58 C. Wang, M. M. Zieger, A. Schenzel, M. Wegener, J. Willenbacher, C. Barner-Kowollik and C. N. Bowman, *Adv. Funct. Mater.*, 2017, **27**, 1605317.

59 S. M. Hashemnejad, A. Z. M. Badruddoza, B. Zarket, C. Ricardo Castaneda and P. S. Doyle, *Nat. Commun.*, 2019, **10**, 2749.

60 L.-C. Cheng, Z. M. Sherman, J. W. Swan and P. S. Doyle, *Langmuir*, 2019, **35**, 9464–9473.

61 Q. Zhang, W.-J. Wang, Y. Lu, B.-G. Li and S. Zhu, *Macromolecules*, 2011, **44**, 6539–6545.

62 M. Motornov, Y. Roiter, I. Tokarev and S. Minko, *Prog. Polym. Sci.*, 2010, **35**, 174–211.

63 X. Liu, Y. Yang and M. W. Urban, *Macromol. Rapid Commun.*, 2017, **38**, 1700030.

64 R. Partch, E. Matijević, A. W. Hodgson and B. E. Aiken, *J. Polym. Sci. Polym. Chem. Ed.*, 1983, **21**, 961–967.

65 J. Wang, B. Li, Q. Jin, X. Huang, J. Shen and C. Kan, *Des. Monomers Polym.*, 2015, **18**, 611–619.

66 Y. Hu, B. Shen, B. Li, M. Xu, G. Jiang and C. Kan, *RSC Adv.*, 2016, **6**, 37765–37772.

67 B. Li, W. Shao, Y. Wang, D. Xiao, C. Li and C. Kan, *Prog. Org. Coatings*, 2019, **129**, 140–146.

68 B. Li, J. Shen, W. Ji, G. Cheng and C. Kan, *Chinese J. Chem.*, 2012, **30**, 2338–2342.

69 C. Schaller, D. Rogez and A. Braig, *J. Coatings Technol. Res.*, 2012, **9**, 433–441.

70 D. Nguyen, H. S. Zondanos, J. M. Farrugia, A. K. Serelis, C. H. Such and B. S. Hawkett, *Langmuir*, 2008, **24**, 2140–2150.

71 M. Aguirre, M. Paulis and J. R. Leiza, *J. Mater. Chem. A*, 2013, **1**, 3155–3162.

72 M. Xiong, G. Gu, B. You and L. Wu, *J. Appl. Polym. Sci.*, 2003, **90**, 1923–1931.

73 J. Garnier, J. Warnant, P. Lacroix-Desmazes, P.-E. Dufils, J. Vinas, Y. Vanderveken and A. M. van Herk, *Macromol. Rapid Commun.*, 2012, **33**, 1388–1392.

74 N. Zgheib, J.-L. Putaux, A. Thill, E. Bourgeat-Lami, F. D'Agosto and M. Lansalot, *Polym. Chem.*, 2013, **4**, 607–614.

75 I. Martín-Fabiani, M. L. Koh, F. Dalmas, K. L. Elidottir, S. J. Hinder, I. Jurewicz, M. Lansalot, E. Bourgeat-Lami and J. L. Keddie, *ACS Appl. Nano Mater.*, 2018, **1**, 3956–3968.

76 M. Irie, *Chem. Rev.*, 2000, **100**, 1683–1684.

77 L. Kortekaas and W. R. Browne, *Chem. Soc. Rev.*, 2019, **48**, 3406–3424.

78 A. Abdollahi, H. Roghani-Mamaqani and B. Razavi, *Prog. Polym. Sci.*, 2019, **98**, 101149.

79 R. Klajn, *Chem. Soc. Rev.*, 2014, **43**, 148–184.

80 J. Su, J. Chen, F. Zeng, Q. Chen, S. Wu and Z. Tong, *Polym. Bull.*, 2008, **61**, 425–434.

81 A. Abdollahi, A. R. Mahdavian and H. Salehi-Mobarakeh, *Langmuir*, 2015, **31**, 10672–10682.

82 F. Khakzad, A. R. Mahdavian, H. Salehi-Mobarakeh, A. Rezaee Shirin-Abadi and M. Cunningham, *Polymer (Guildf).*,

2016, **101**, 274–283.

83 A. Abdollahi, J. K. Rad and A. R. Mahdavian, *Carbohydr. Polym.*, 2016, **150**, 131–138.

84 A. Abdollahi, A. Herizchi, H. Roghani-Mamaqani and H. Alidaei-Sharif, *Carbohydr. Polym.*, 2019, 115603.

85 A. Abdollahi, K. Sahandi-Zangabad and H. Roghani-Mamaqani, *ACS Appl. Mater. Interfaces*, 2018, **10**, 39279–39292.

86 C. R. Ronda, *Luminescence*, 2007, 1–34.

87 X. Li, C. Li, S. Wang, H. Dong, X. Ma and D. Cao, *Dye. Pigment.*, 2017, **142**, 481–490.

88 W. Li, Z. Qiu, M. Tebyetekerwa, J. Zhang, Y. Wang, T. Gao, J. Wang, Y. Ding and Y. Xie, *Prog. Org. Coatings*, 2019, **127**, 8–15.

89 X. Liang, Y. Hu, Z. Cao, L. Xiao, J. Lou, L. Liu, Y. Wang, Z. Zhao, D. Qi and Q. Cui, *Dye. Pigment.*, 2019, **163**, 371–380.

90 X. Liang, Y. Hu, J. Lou, Z. Cao, L. Liu, Y. Wang, Z. Zhao, D. Qi and Q. Cui, *Dye. Pigment.*, 2019, **160**, 572–578.

91 M.-Q. Zhu, G.-F. Zhang, Z. Hu, M. P. Aldred, C. Li, W.-L. Gong, T. Chen, Z.-L. Huang and S. Liu, *Macromolecules*, 2014, **47**, 1543–1552.

92 J. Keyvan Rad, A. R. Mahdavian, S. Khoei and A. Janati Esfahani, *Polymer (Guildf).*, 2016, **98**, 263–269.

93 K. Yin Win and S.-S. Feng, *Biomaterials*, 2005, **26**, 2713–2722.

94 K. J. Lee, W.-K. Oh, J. Song, S. Kim, J. Lee and J. Jang, *Chem. Commun.*, 2010, **46**, 5229–5231.

95 Y. Zhao, C. Shi, X. Yang, B. Shen, Y. Sun, Y. Chen, X. Xu, H. Sun, K. Yu, B. Yang and Q. Lin, *ACS Nano*, 2016, **10**, 5856–5863.

96 M. Bradley, M. Ashokkumar and F. Grieser, *J. Am. Chem. Soc.*, 2003, **125**, 525–529.

97 M. Probes, *Prod. information, Mol. Probes*.

98 G. Bosma, C. Pathmamanoharan, E. H. A. de Hoog, W. K. Kegel, A. van Blaaderen and H. N. W. Lekkerkerker, *J. Colloid Interface Sci.*, 2002, **245**, 292–300.

99 R. S. Jardine and P. Bartlett, *Colloids Surfaces A Physicochem. Eng. Asp.*, 2002, **211**, 127–132.

100 R. P. A. Dullens, E. M. Claesson and W. K. Kegel, *Langmuir*, 2004, **20**, 658–664.

101 C. Tu, Y. Yang and M. Gao, *Nanotechnology*, 2008, **19**, 105601.

102 W. Li, J. Wang, Y. Xie, M. Tebyetekerwa, Z. Qiu, J. Tang, S. Yang, M. Zhu and Z. Xu, *Prog. Org. Coatings*, 2018, **120**, 1–9.

103 J. Keyvan Rad and A. R. Mahdavian, *Eur. Polym. J.*, 2017, **88**, 56–66.

104 Y. Zhu, I. Heim and B. Tieke, *Macromol. Chem. Phys.*, 2006, **207**, 2206–2214.

105 S. Bretler, U. Bretler and S. Margel, *Eur. Polym. J.*, 2017, **89**, 13–22.

106 S. Bretler and S. Margel, *Polymer (Guildf).*, 2015, **61**, 68–74.

107 A. Abdollahi, K. Sahandi-Zangabad and H. Roghani-Mamaqani, *Langmuir*, 2018, **34**, 13910–13923.

108 R. Sauer, A. Turshatov, S. Baluschev and K. Landfester, *Macromolecules*, 2012, **45**, 3787–3796.

109 C. Wang, S. Chatani, M. Podgórski and C. N. Bowman, *Polym. Chem.*, 2015, **6**, 3758–3763.

110 J. Keyvan Rad, A. R. Mahdavian, H. Salehi-Mobarakeh and A. Abdollahi, *Macromolecules*, 2016, **49**, 141–152.

111 A. I. Campbell and P. Bartlett, *J. Colloid Interface Sci.*, 2002, **256**, 325–330.

112 K. Ando and H. Kawaguchi, *J. Colloid Interface Sci.*, 2005, **285**, 619–626.

113 T. Tamai, M. Watanabe, H. Maeda and K. Mizuno, *J. Polym. Sci. Part A Polym. Chem.*, 2008, **46**, 1470–1475.

114 V. Holzapfel, M. Lorenz, C. K. Weiss, H. Schrezenmeier, K. Landfester and V. Mailänder, *J. Phys. Condens. Matter*, 2006, **18**, S2581–S2594.

115 H.-Y. Xie, C. Zuo, Y. Liu, Z.-L. Zhang, D.-W. Pang, X.-L. Li, J.-P. Gong, C. Dickinson and W. Zhou, *Small*, 2005, **1**, 506–509.

116 M. Han, X. Gao, J. Z. Su and S. Nie, *Nat. Biotechnol.*, 2001, **19**, 631–635.

117 H. Xu, M. Y. Sha, E. Y. Wong, J. Uphoff, Y. Xu, J. A. Treadway, A. Truong, E. O'Brien, S. Asquith, M. Stubbins, N. K. Spurr, E. H. Lai and W. Mahoney, *Nucleic Acids Res.*, 2003, **31**, e43–e43.

118 D. Wang, A. L. Rogach and F. Caruso, *Nano Lett.*, 2002, **2**, 857–861.

119 A. S. Susha, F. Caruso, A. L. Rogach, G. B. Sukhorukov, A. Kornowski, H. Möhwald, M. Giersig, A. Eychmüller and H. Weller, *Colloids Surfaces A Physicochem. Eng. Asp.*, 2000, **163**, 39–44.

120 A. Rogach, A. Susha, F. Caruso, G. Sukhorukov, A. Kornowski, S. Kershaw, H. Möhwald, A. Eychmüller and H. Weller, *Adv. Mater.*, 2000, **12**, 333–337.

121 I. L. Radtchenko, G. B. Sukhorukov, N. Gaponik, A. Kornowski, A. L. Rogach and H. Möhwald, *Adv. Mater.*, 2001, **13**, 1684–1687.

122 N. Gaponik, I. L. Radtchenko, M. R. Gerstenberger, Y. A. Fedutik, G. B. Sukhorukov and A. L. Rogach, *Nano Lett.*, 2003, **3**, 369–372.

123 N. Joumaa, M. Lansalot, A. Théretz, A. Elaissari, A. Sukhanova, M. Artemyev, I. Nabiev and J. H. M. Cohen, *Langmuir*, 2006, **22**, 1810–1816.

124 N. Tomczak, D. Jańczewski, M. Han and G. J. Vancso, *Prog. Polym. Sci.*, 2009, **34**, 393–430.

125 M.-Q. Zhu, L. Zhu, J. J. Han, W. Wu, J. K. Hurst and A. D. Q. Li, *J. Am. Chem. Soc.*, 2006, **128**, 4303–4309.

126 J. Chen, F. Zeng, S. Wu, J. Su and Z. Tong, *Small*, 2009, **5**,

970–978.

127 F. Tronc, M. Li, J. Lu, M. A. Winnik, B. L. Kaul and J.-C. Graciet, *J. Polym. Sci. Part A Polym. Chem.*, 2003, **41**, 766–778.

128 J. B. Birks, *Aromatic Molecules*, Wiley: New York, 1970, vol. 704.

129 D. Ding, K. Li, B. Liu and B. Z. Tang, *Acc. Chem. Res.*, 2013, **46**, 2441–2453.

130 J. Luo, Z. Xie, J. W. Y. Lam, L. Cheng, H. Chen, C. Qiu, H. S. Kwok, X. Zhan, Y. Liu, D. Zhu and B. Z. Tang, *Chem. Commun.*, 2001, 1740–1741.

131 X. Zhang, X. Zhang, B. Yang, M. Liu, W. Liu, Y. Chen and Y. Wei, *Polym. Chem.*, 2014, **5**, 399–404.

132 M. Liu, X. Zhang, B. Yang, F. Deng, Z. Li, J. Wei, X. Zhang and Y. Wei, *Appl. Surf. Sci.*, 2014, **322**, 155–161.

133 Z. Cao, X. Liang, H. Chen, M. Gao, Z. Zhao, X. Chen, C. Xu, G. Qu, D. Qi and B. Z. Tang, *Polym. Chem.*, 2016, **7**, 5571–5578.

134 Z. Cao, C. Xu, L. Liang, Z. Zhao, B. Chen, Z. Chen, H. Chen, G. Qu, D. Qi, G. Shan and U. Ziener, *Polym. Chem.*, 2015, **6**, 6378–6385.

135 G. A. Jones and D. S. Bradshaw, *Front. Phys.* , 2019, 7, 100.

136 B. L. Sanchez-Gaytan, F. Fay, S. Hak, A. Alaarg, Z. A. Fayad, C. Perez-Medina, W. J. M. Mulder and Y. Zhao, *Angew. Chemie*, 2017, **129**, 2969–2972.

137 K. Truong and M. Ikura, *Curr. Opin. Struct. Biol.*, 2001, **11**, 573–578.

138 C. Le Zhao, Y. Wang, Z. Hruska and M. A. Winnik, *Macromolecules*, 1990, **23**, 4082–4087.

139 G. R. Bardajee, C. Vancaeyzeele, J. C. Haley, A. Y. Li and M. A. Winnik, *Polymer (Guildf).*, 2007, **48**, 5839–5849.

140 J. C. Haley, Y. Liu, M. A. Winnik and W. Lau, *J. Coatings Technol. Res.*, 2008, **5**, 157–168.

141 M. Soleimani, S. Khan, D. Mendenhall, W. Lau and M. A. Winnik, *Polymer (Guildf).*, 2012, **53**, 2652–2663.

142 W. F. Schroeder, Y. Liu, J. P. Tomba, M. Soleimani, W. Lau and M. A. Winnik, *Polymer (Guildf).*, 2011, **52**, 3984–3993.

143 J. K. Oh, P. Tomba, X. Ye, R. Eley, J. Rademacher, R. Farwaha and M. A. Winnik, *Macromolecules*, 2003, **36**, 5804–5814.

144 E. González, M. J. Barandiaran and M. Paulis, *Prog. Org. Coatings*, 2015, **88**, 137–143.

145 K. González-Matheus, G. P. Leal and J. M. Asua, *Polymer (Guildf).*, 2015, **69**, 73–82.

146 L. Cerdán, E. Enciso, V. Martín, J. Bañuelos, I. López-Arbeloa, A. Costela and I. García-Moreno, *Nat. Photonics*, 2012, **6**, 621–626.

147 P. Hess and J. Pelzl, *Photoacoustic and Photothermal Phenomena, Volume 58*, Springer-Verlag, Berlin, Heidelberg, 1987.

148 J. Wu, T. Kitamori and T. Sawada, *J. Appl. Phys.*, 1991, **69**, 7015–7020.

149 T. Kitamori and T. Sawada, *Polym. Int.*, 1993, **30**, 451–453.

150 K. Mawatari, T. Kitamori and T. Sawada, *Anal. Chem.*, 1998, **70**, 5037–5041.

151 T. Kitamori, K. Suzuki, K. Yokose, T. Sawada, A. Harada and Y. Gohshi, eds. P. Hess and J. Pelzl, Springer Berlin Heidelberg, Berlin, Heidelberg, 1988, pp. 150–151.

152 T. S. Thomas, P. S. Dale, R. M. Weight, U. Atasoy, J. Magee and J. A. Viator, in *Proc. SPIE 6856, Photons Plus Ultrasound: Imaging and Sensing 2008: The Ninth Conference on Biomedical Thermoacoustics, Optoacoustics, and Acoustooptics*, 2008, p. 685609.

153 M. Mehrmohammadi, S. J. Yoon, D. Yeager and S. Y. Emelianov, *Curr. Mol. Imaging*, 2013, **2**, 89–105.

154 C. L. Bayer, P. P. Joshi and S. Y. Emelianov, *Expert Rev. Med. Devices*, 2013, **10**, 125–134.

155 V. Shanmugam, S. Selvakumar and C.-S. Yeh, *Chem. Soc. Rev.*, 2014, **43**, 6254–6287.

156 M. Asadian-Birjand, J. Bergueiro, S. Wedepohl and M. Calderón, *Macromol. Biosci.*, 2016, **16**, 1432–1441.

157 M. Molina, S. Wedepohl and M. Calderón, *Nanoscale*, 2016, **8**, 5852–5856.

158 L. E. Strong, S. N. Dahotre and J. L. West, *J. Control. Release*, 2014, **178**, 63–68.

159 R. Chang and W.-B. Tsai, *Polymers (Basel).*, 2018, **10**, 1098.

160 X. Shen, T. Li, Z. Chen, X. Xie, H. Zhang, Y. Feng, S. Li, X. Qin, H. Yang, C. Wu, C. Zheng, J. Zhu, F. You and Y. Liu, *Mol. Pharm.*, 2019, **16**, 1367–1384.

161 F. Ding, X. Gao, X. Huang, H. Ge, M. Xie, J. Qian, J. Song, Y. Li, X. Zhu and C. Zhang, *Biomaterials*, 2020, **245**, 119976.

162 B. Shang, M. Chen and L. Wu, *Small*, 2019, **15**, 1901888.

163 X. Xu, B. Bai, H. Wang and Y. Suo, *ACS Appl. Mater. Interfaces*, 2017, **9**, 6424–6432.

164 K. Nakata and A. Fujishima, *J. Photochem. Photobiol. C Photochem. Rev.*, 2012, **13**, 169–189.

165 N. S. Allen, M. Edge, G. Sandoval, J. Verran, J. Stratton and J. Maltby, *Photochem. Photobiol.*, 2005, **81**, 279–290.

166 W. A. Lee, N. Pernodet, B. Li, C. H. Lin, E. Hatchwell and M. H. Rafailovich, *Chem. Commun.*, 2007, 4815–4817.

167 J. Xiao, W. Chen, F. Wang and J. Du, *Macromolecules*, 2013, **46**, 375–383.

168 S. Livraghi, I. Corazzari, M. C. Paganini, G. Ceccone, E. Giamello, B. Fubini and I. Fenoglio, *Chem. Commun.*, 2010, **46**, 8478–8480.

169 M. Morsella, M. Giammatteo, L. Arrizza, L. Tonucci, M. Bressan and N. d'Alessandro, *RSC Adv.*, 2015, **5**, 57453–57461.

170 L. Caballero, K. A. Whitehead, N. S. Allen and J. Verran, *Dye. Pigment.*, 2010, **86**, 56–62.

171 E. González, A. Bonnefond, M. Barrado, A. M. Casado

Barrasa, J. M. Asua and J. R. Leiza, *Chem. Eng. J.*, 2015, **281**, 209–217.

172 L. Yang, S. Zhou and L. Wu, *Prog. Org. Coatings*, 2015, **85**, 208–215.

173 F. Xu, T. Wang, H. Chen, J. Bohling, A. M. Maurice, L. Wu and S. Zhou, *Prog. Org. Coatings*, 2017, **113**, 15–24.

174 R. Nosrati, A. Olad and H. Najjari, *Surf. Coatings Technol.*, 2017, **316**, 199–209.

175 T. Martinez, A. Bertron, E. Ringot and G. Escadeillas, *Build. Environ.*, 2011, **46**, 1808–1816.

176 A. Bonnefond, E. González, M. J. Asua, R. J. Leiza, E. Ieva, G. Brinati, S. Carella, A. Marrani, A. Veneroni, J. Kiwi, C. Pulgarin and S. Rtimi, *Cryst.* , 2016, 6.

177 X.-C. Che, Y.-Z. Jin and Y.-S. Lee, *Prog. Org. Coatings*, 2010, **69**, 534–538.

178 A. Bonnefond, E. González, J. M. Asua, J. R. Leiza, J. Kiwi, C. Pulgarin and S. Rtimi, *Colloids Surfaces B Biointerfaces*, 2015, **135**, 1–7.

179 M. Baudys, J. Krýsa, M. Zlámal and A. Mills, *Chem. Eng. J.*, 2015, **261**, 83–87.

180 L. Hochmannova and J. Vytrasova, *Prog. Org. Coatings*, 2010, **67**, 1–5.

181 J. Li, C. Nagamani and J. S. Moore, *Acc. Chem. Res.*, 2015, **48**, 2181–2190.

182 H. M. D. Bandara and S. C. Burdette, *Chem. Soc. Rev.*, 2012, **41**, 1809–1825.

183 Y. Li, Y. He, X. Tong and X. Wang, *J. Am. Chem. Soc.*, 2005, **127**, 2402–2403.

184 Y. Li, Y. He, X. Tong and X. Wang, *Langmuir*, 2006, **22**, 2288–2291.

185 J. Kumar, L. Li, X. L. Jiang, D.-Y. Kim, T. S. Lee and S. Tripathy, *Appl. Phys. Lett.*, 1998, **72**, 2096–2098.

186 R. H. Lambeth and J. S. Moore, *Macromolecules*, 2007, **40**, 1838–1842.

187 N. Li, G. Ye, Y. He and X. Wang, *Chem. Commun.*, 2011, **47**, 4757–4759.

188 Y. Zhou and X. G. Wang, *Macromol. Chem. Phys.*, 2015, **216**, 2040–2047.

189 X. Zhou, Y. Du and X. Wang, *ACS Macro Lett.*, 2016, **5**, 234–237.

190 B. Liu, Y. Zhou, X. Zhou and X. Wang, *Macromol. Chem. Phys.*, 2017, **218**, 1700020.

191 C. Hsu, Y. Du and X. Wang, *Langmuir*, 2017, **33**, 10645–10654.

192 X. Hou, S. Guan, T. Qu, X. Wu, D. Wang, A. Chen and Z. Yang, *ACS Macro Lett.*, 2018, **7**, 1475–1479.

193 J. Lee, K. H. Ku, J. Kim, Y. J. Lee, S. G. Jang and B. J. Kim, *J. Am. Chem. Soc.*, 2019, **141**, 15348–15355.

194 E. M. Verdurmen, J. G. Albers and A. L. German, *Colloid Polym. Sci.*, 1994, **272**, 57–63.

195 X. Su, C. Fowler, C. O'Neill, J. Pinaud, E. Kowal, P. Jessop and M. Cunningham, *Macromol. Symp.*, 2013, **333**, 93–101.

196 S.-C. Ng and L.-H. Gan, *Eur. Polym. J.*, 1981, **17**, 1073–1077.

197 W. G. Barb and W. Mikucki, *J. Polym. Sci.*, 1959, **37**, 499–514.

198 R. Zimehl and G. Lagaly, ed. J. Springer, Steinkopff, Darmstadt, 1985, pp. 28–36.

199 F. Csempesz and S. Rohrsetzer, *Colloids and Surfaces*, 1988, **31**, 215–230.

200 J. C. Husband and J. M. Adams, *Colloid Polym. Sci.*, 1992, **270**, 1194–1200.

201 M. Mihara, P. Jessop and M. Cunningham, *Macromolecules*, 2011, **44**, 3688–3693.

202 D. H. Napper, *Polymeric stabilization of colloidal dispersions*, Academic Press, London, UK, 1983.

203 R. M. Fitch, *Polymer Colloids: A Comprehensive Introduction*, Academic Press, London, UK, 1997.

204 Jacob N. Israelachvili, *Intermolecular and Surface Forces*, Elsevier Inc., 3rd edn., 2011.

205 M. Sanchez-Dominguez, P. Wyatt and J. Eastoe, in *Self Assembly*, Ios Pr Inc, 2003.

206 A. Mamane, E. Chevallier, L. Olanier, F. Lequeux and C. Monteux, *Soft Matter*, 2017, **13**, 1299–1305.

207 L. Yang, N. Takisawa, T. Hayashita and K. Shirahama, *J. Phys. Chem.*, 1995, **99**, 8799–8803.

208 Y. Takahashi, K. Fukuyasu, T. Horiuchi, Y. Kondo and P. Stroeve, *Langmuir*, 2014, **30**, 41–47.

209 F. Jasinski, T. R. Guimarães, S. David, C. Suniary, T. Funston, Y. Takahashi, Y. Kondo and P. B. Zetterlund, *Macromol. Rapid Commun.*, 2019, **40**, 1900355.

210 X. Yuan, K. Fischer and W. Schärtl, *Adv. Funct. Mater.*, 2004, **14**, 457–463.

211 R. Mukhopadhyay, S. K. De and S. N. Chakraborty, *Polymer (Guildf).*, 1977, **18**, 1243–1249.

212 M. Akiba and A. S. Hashim, *Prog. Polym. Sci.*, 1997, **22**, 475–521.

213 F. Masson, C. Decker, T. Jaworek and R. Schwalm, *Prog. Org. Coatings*, 2000, **39**, 115–126.

214 S. Y. Chee and S. N. Gan, *J. Appl. Polym. Sci.*, 2006, **100**, 2317–2322.

215 M. Hirose, J. Zhou and F. Kadowaki, *Colloids Surfaces A Physicochem. Eng. Asp.*, 1999, **153**, 481–485.

216 M. Visconti and M. Cattaneo, *Prog. Org. Coatings*, 2000, **40**, 243–251.

217 Z. Wang, D. Gao, J. Yang and Y. Chen, *J. Appl. Polym. Sci.*, 1999, **73**, 2869–2876.

218 G. Ye, F. Courtecuisse, X. Allonas, C. Ley, C. Croutxe-Barghorn, P. Raja, P. Taylor and G. Bescond, *Prog. Org.*

Coatings, 2012, **73**, 366–373.

219 W. J. Muizebelt, J. C. Hubert, M. W. F. Nielen, R. P. Klaasen and K. H. Zabel, *Prog. Org. Coatings*, 2000, **40**, 121–130.

220 J. W. Taylor and M. A. Winnik, *JCT Res.*, 2004, **1**, 163–190.

221 E. F. Assanvo and S. D. Baruah, *Prog. Org. Coatings*, 2015, **86**, 25–32.

222 C. Y. Bai, X. Y. Zhang, J. B. Dai and W. H. Li, *Prog. Org. Coatings*, 2006, **55**, 291–295.

223 Z. Wang, D. Gao, J. Yang and Y. Chen, *J. Appl. Polym. Sci.*, 1999, **73**, 2869–2876.

224 Y. B. Kim, H. K. Kim, J. K. Yoo and J. W. Hong, *Surf. Coatings Technol.*, 2002, **157**, 40–46.

225 K.-D. Suh, Y. S. Chon and J. Y. Kim, *Polym. Bull.*, 1997, **38**, 287–294.

226 J. Odeberg, J. Rassing, J.-E. Jönsson and B. Wesslén, *J. Appl. Polym. Sci.*, 1996, **62**, 435–445.

227 S. Chen and X. Y. Li, *J. Coatings Technol. Res.*, 2008, **5**, 439–445.

228 Y. Yamamoto, P. Suksawad, N. Pukkate, T. Horimai, O. Wakisaka and S. Kawahara, *J. Polym. Sci. Part A Polym. Chem.*, 2010, **48**, 2418–2424.

229 N. Pukkate, T. Horimai, O. Wakisaka, Y. Yamamoto and S. Kawahara, *J. Polym. Sci. Part A Polym. Chem.*, 2009, **47**, 4111–4118.

230 A. Badía, J. I. Santos, A. Agirre, M. J. Barandiaran and J. R. Leiza, *ACS Sustain. Chem. Eng.*, , DOI:10.1021/acssuschemeng.9b05067.

231 S.-H. Kim, S. Y. Lee, S.-M. Yang and G.-R. Yi, *NPG Asia Mater.*, 2011, **3**, 25–33.

232 S. Furumi, *Nanoscale*, 2012, **4**, 5564–5571.

233 E. Tian, L. Cui, J. Wang, Y. Song and L. Jiang, *Macromol. Rapid Commun.*, 2009, **30**, 509–514.

234 P. F. Jacobs, *Rapid prototyping & manufacturing: fundamentals of stereolithography*, Society of Manufacturing Engineers, 1992.

235 A. Zillessen and E. Bartsch, *Langmuir*, 2010, **26**, 89–96.

236 H. Misawa, K. Sasaki, M. Koshioka, N. Kitamura and H. Masuhara, *Macromolecules*, 1993, **26**, 282–286.

237 J. J. Benkoski, R. L. Jones, J. F. Douglas and A. Karim, *Langmuir*, 2007, **23**, 3530–3537.

238 S. Ito, H. Yoshikawa and H. Masuhara, *Appl. Phys. Lett.*, 2001, **78**, 2566–2568.

239 D. Marksteiner, S. Wasser and W. Schärtl, *Langmuir*, 2009, **25**, 12843–12846.

240 C. J. Thrasher, J. J. Schwartz and A. J. Boydston, *ACS Appl. Mater. Interfaces*, 2017, **9**, 39708–39716.

241 D. K. Patel, A. H. Sakhaei, M. Layani, B. Zhang, Q. Ge and S. Magdassi, *Adv. Mater.*, 2017, 1606000-n/a.

242 J. P. Rolland, *J. Photopolym. Sci. Technol.*, 2016, **29**, 451–452.

243 E. M. Wilts, A. M. Pekkanen, B. T. White, V. Meenakshisundaram, D. C. Aduba, C. B. Williams and T. E. Long, *Polym. Chem.*, , DOI:10.1039/C8PY01792A.

244 M. Hegde, V. Meenakshisundaram, N. Chartrain, S. Sekhar, D. Tafti, C. B. Williams and T. E. Long, *Adv. Mater.*, 2017, **29**, 1701240-n/a.

245 J. M. Sirrine, V. Meenakshisundaram, N. G. Moon, P. J. Scott, R. J. Mondschein, T. F. Weiseman, C. B. Williams and T. E. Long, *Polymer (Guildf).*, 2018, **152**, 25–34.

246 P. J. Scott, V. Meenakshisundaram, N. A. Chartrain, J. M. Sirrine, C. B. Williams and T. E. Long, *ACS Appl. Polym. Mater.*, 2019, **1**, 684–690.

247 C. Zhu, A. J. Pascall, N. Dudukovic, M. A. Worsley, J. D. Kuntz, E. B. Duoss and C. M. Spadaccini, *Annu. Rev. Chem. Biomol. Eng.*, 2019, **10**, 17–42.

248 M. E. Helgeson, S. E. Moran, H. Z. An and P. S. Doyle, *Nat. Mater.*, 2012, **11**, 344.

249 Y. Zhang, M.-J. Yin, X. Ouyang, A. P. Zhang and H.-Y. Tam, *Appl. Mater. Today*, 2020, **19**, 100580.

250 2016.

251 3D Printing with PTFE, https://www.3m.com/3M/en_US/design-and-specialty-materials-us/3d-printing/, (accessed 29 June 2019).

252 F. Kotz, P. Risch, D. Helmer and B. E. Rapp, *Adv. Mater.*, 2019, **31**, 1805982.

253 Y. Xia, B. Gates, Y. Yin and Y. Lu, *Adv. Mater.*, 2000, **12**, 693–713.

254 Y. Zhang, J. Wang, Y. Huang, Y. Song and L. Jiang, *J. Mater. Chem.*, 2011, **21**, 14113–14126.

255 S. Hayashi, Y. Kumamoto, T. Suzuki and T. Hirai, *J. Colloid Interface Sci.*, 1991, **144**, 538–547.

256 D. Klinger and K. Landfester, *Macromol. Rapid Commun.*, 2011, **32**, 1979–1985.

257 D. Klinger and K. Landfester, *Soft Matter*, 2011, **7**, 1426–1440.

258 J. de S. Nunes and J. M. Asua, *Langmuir*, 2012, **28**, 7333–7342.

259 Y. Gu, K. Kawamoto, M. Zhong, M. Chen, M. J. A. Hore, A. M. Jordan, L. T. J. Korley, B. D. Olsen and J. A. Johnson, *Proc. Natl. Acad. Sci.*, 2017, **114**, 4875.

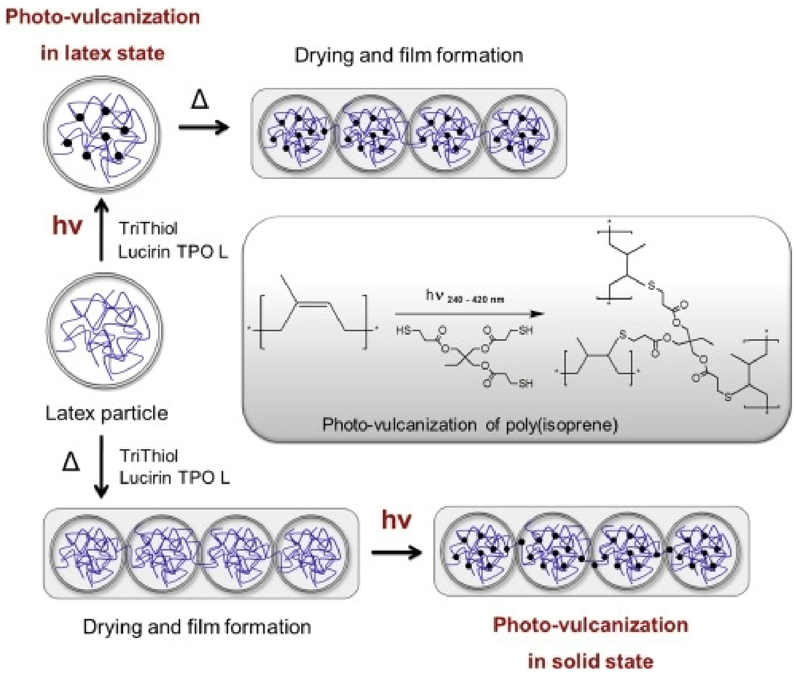
Photo-vulcanization
in latex state
Drying and film formation
Δ
hν
TriThiol
Lucirin TPO L
hν 240 - 420 nm
HS
SH
SH
S
O
Photo-vulcanization of poly(isoprene)
Latex particle
Δ
TriThiol
Lucirin TPO L
hν
Drying and film formation
Photo-vulcanization
in solid state

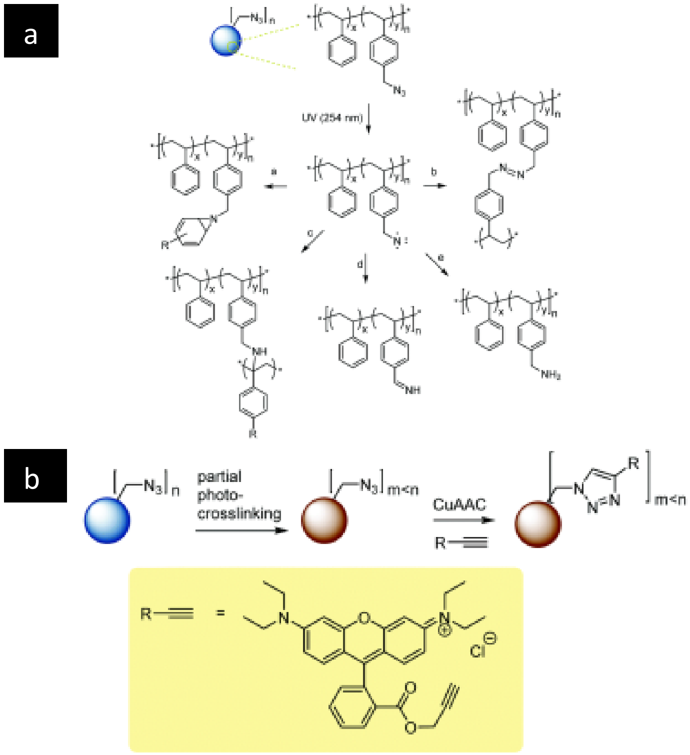
a
N3
n
x
y
n
N3
UV (254 nm)
a
b
c
d
e
N
R
N=N
NH
NH
NH2
R
b
N3
n
partial
photo-
crosslinking
N3
m<n
CuAAC
R
N
N=N
R
m<n
R
=
N
O
N
Cl
O
O

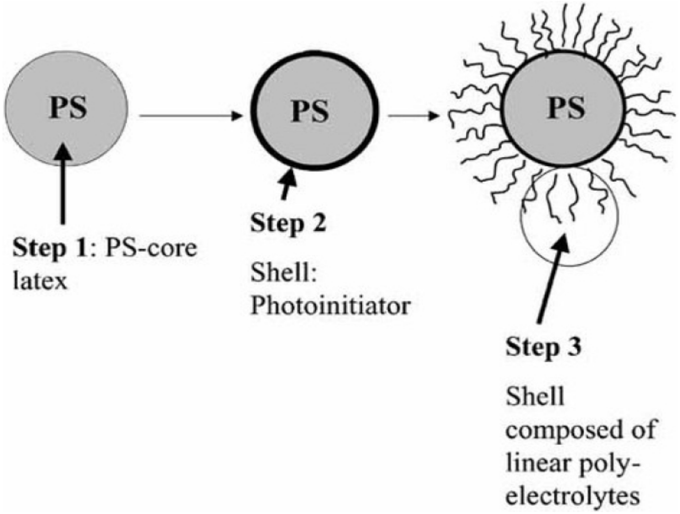
PS
PS
PS
Step 1: PS-core latex
Step 2
Shell: Photoinitiator
Step 3
Shell composed of linear poly-electrolytes

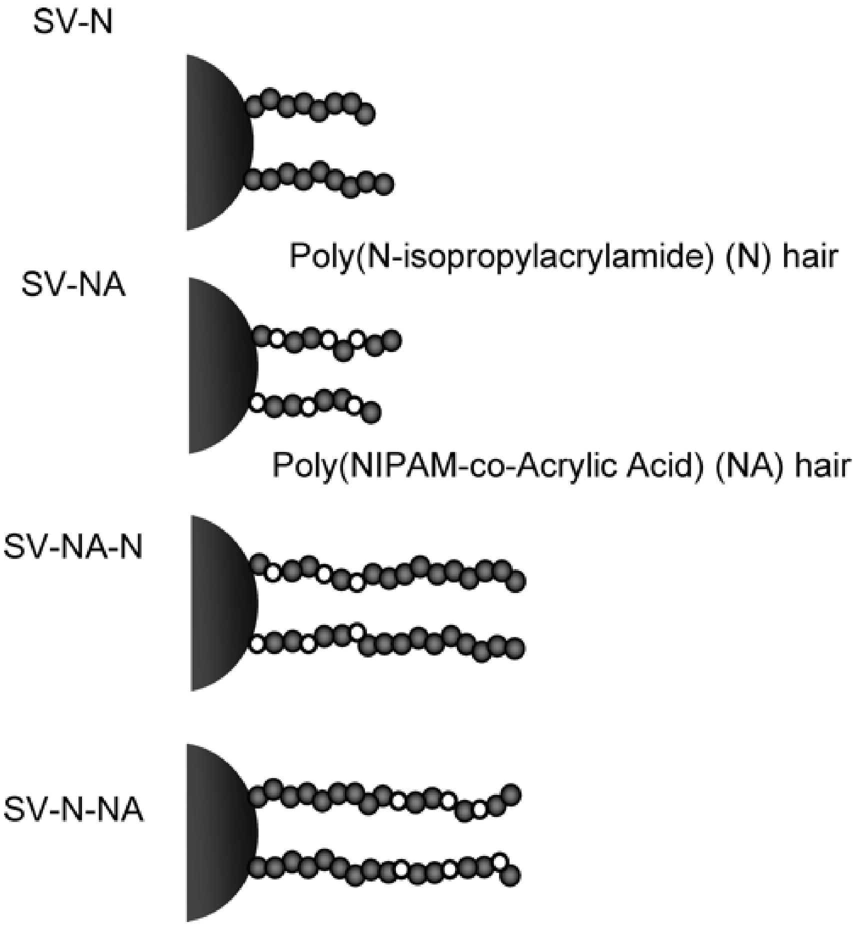
SV-N
Poly(N-isopropylacrylamide) (N) hair
SV-NA
Poly(NIPAM-co-Acrylic Acid) (NA) hair
SV-NA-N
SV-N-NA

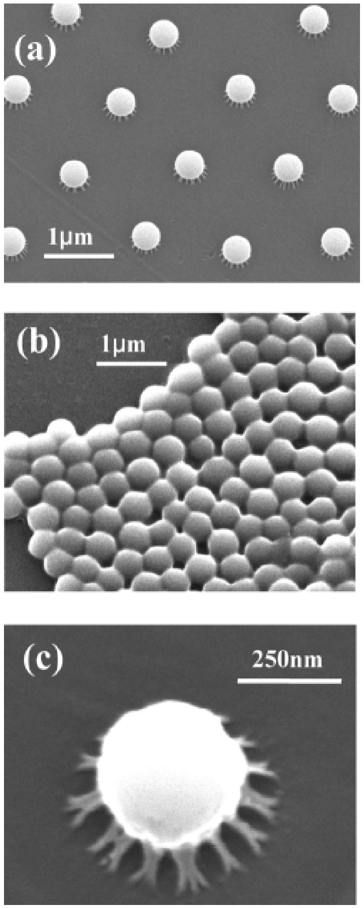
(a)
1μm
(b)
1μm
(c)
250nm

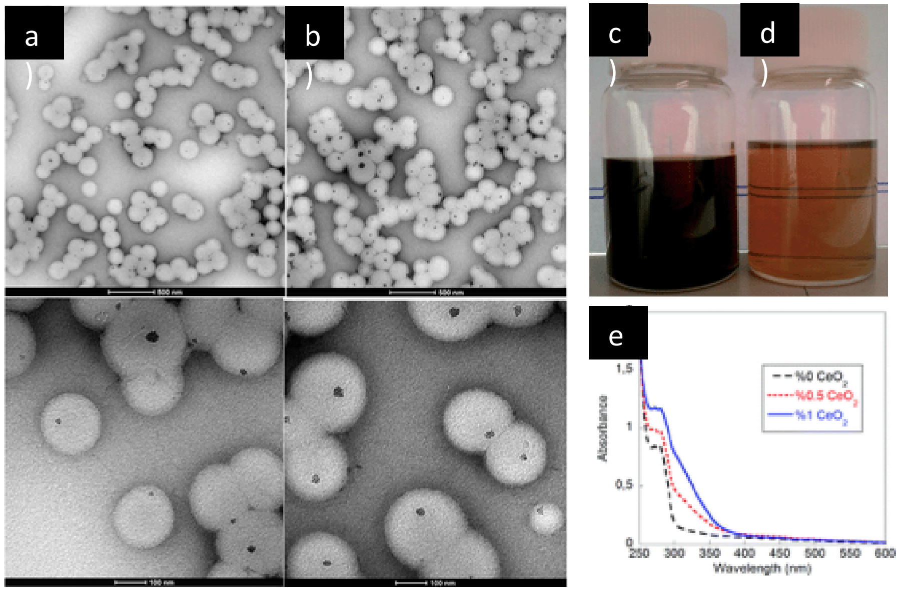
a
)
b
)
500 nm
500 nm
100 nm
100 nm
c
)
d
)
e
%0 CeO$_2$
%0.5 CeO$_2$
%1 CeO$_2$
Absorbance
1,5
1
0,5
0
250
300
350
400
450
500
550
600
Wavelength (nm)

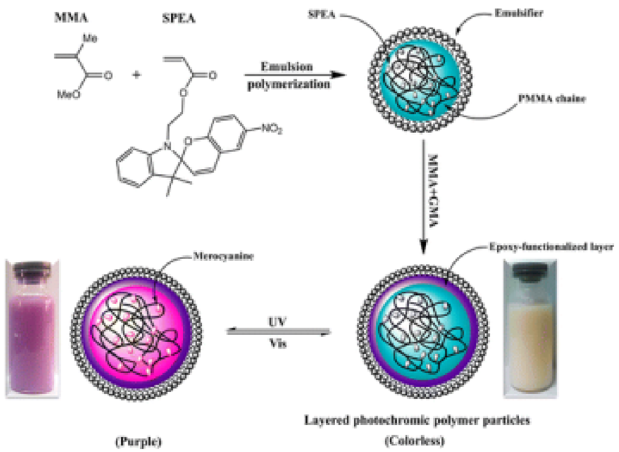
MMA
SPEA
Me
MeO
O
NO2
Emulsion polymerization
SPEA
Emulsifier
PMMA chains
MMA+GMA
Epoxy-functionalized layer
Merocyanine
UV
Vis
(Purple)
Layered photochromic polymer particles
(Colorless)

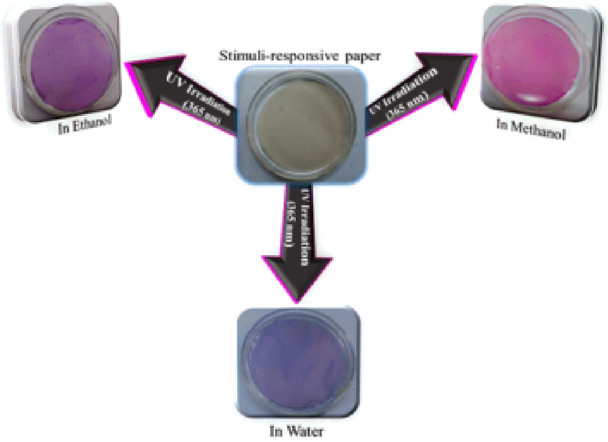
Stimuli-responsive paper
UV irradiation (365 nm)
UV irradiation (365 nm)
UV irradiation (365 nm)
In Ethanol
In Methanol
In Water

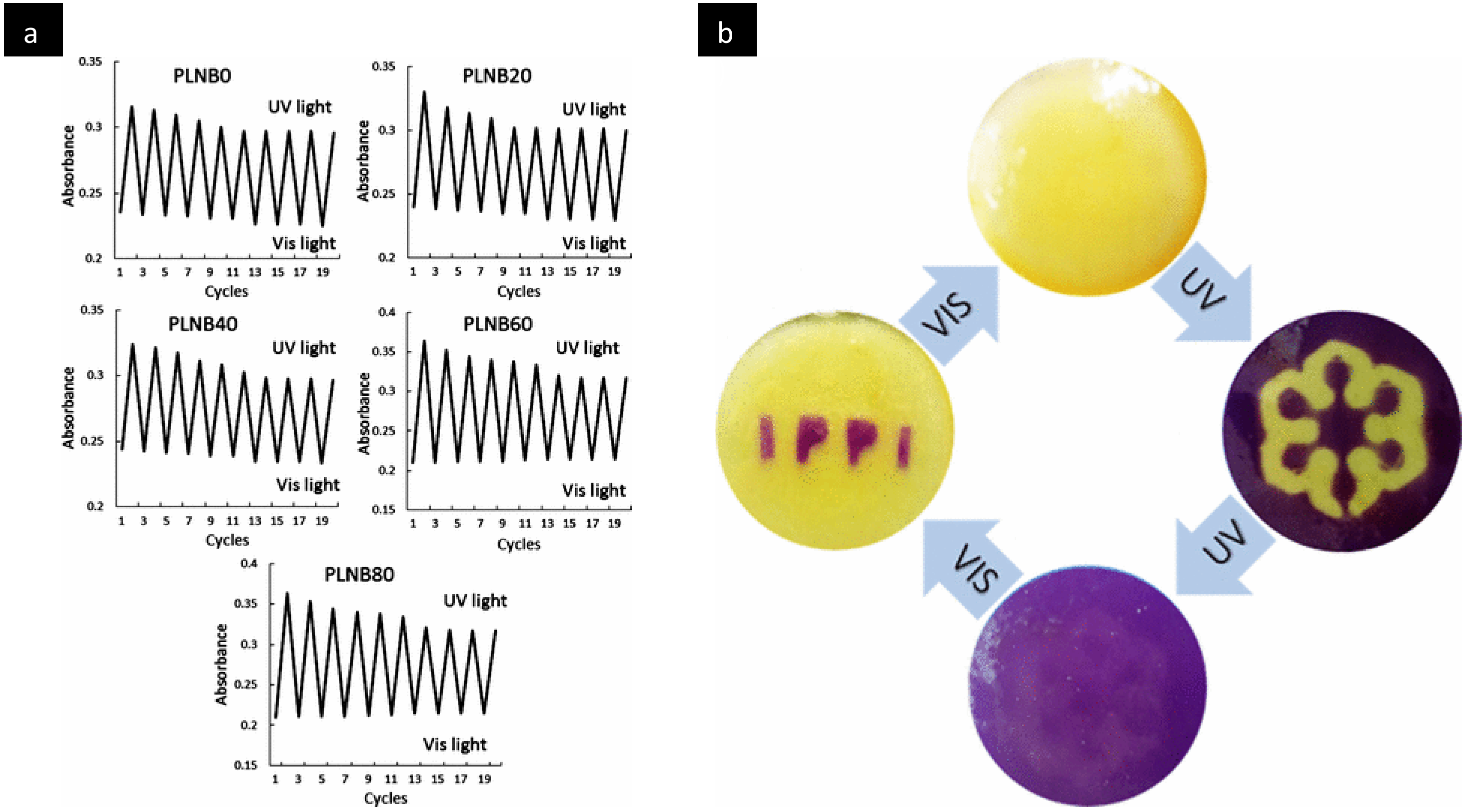
a
PLNB0
PLNB20
PLNB40
PLNB60
PLNB80
UV light
Vis light
Absorbance
Cycles
0.15
0.2
0.25
0.3
0.35
0.4
1 3 5 7 9 11 13 15 17 19
b
VIS
UV
UV
VIS
IPPI

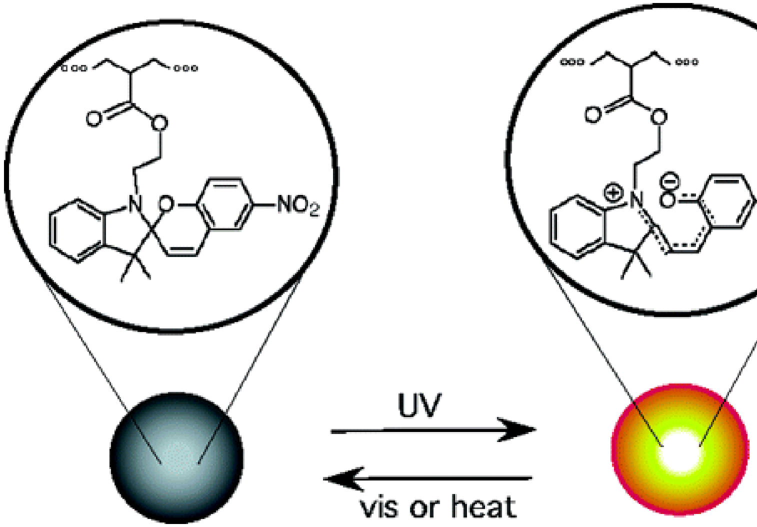
O
O
N
O
NO2
⊕N
⊖O
NO2
UV
vis or heat

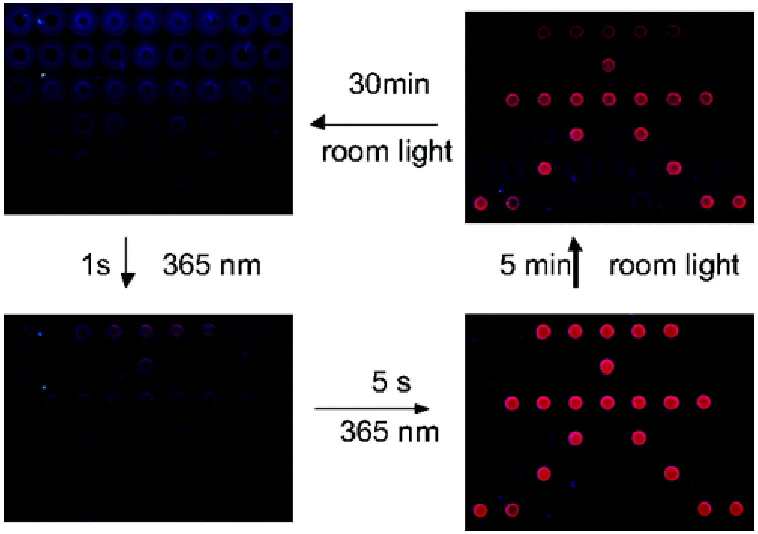
30min
room light
1s
365 nm
5 min
room light
5 s
365 nm

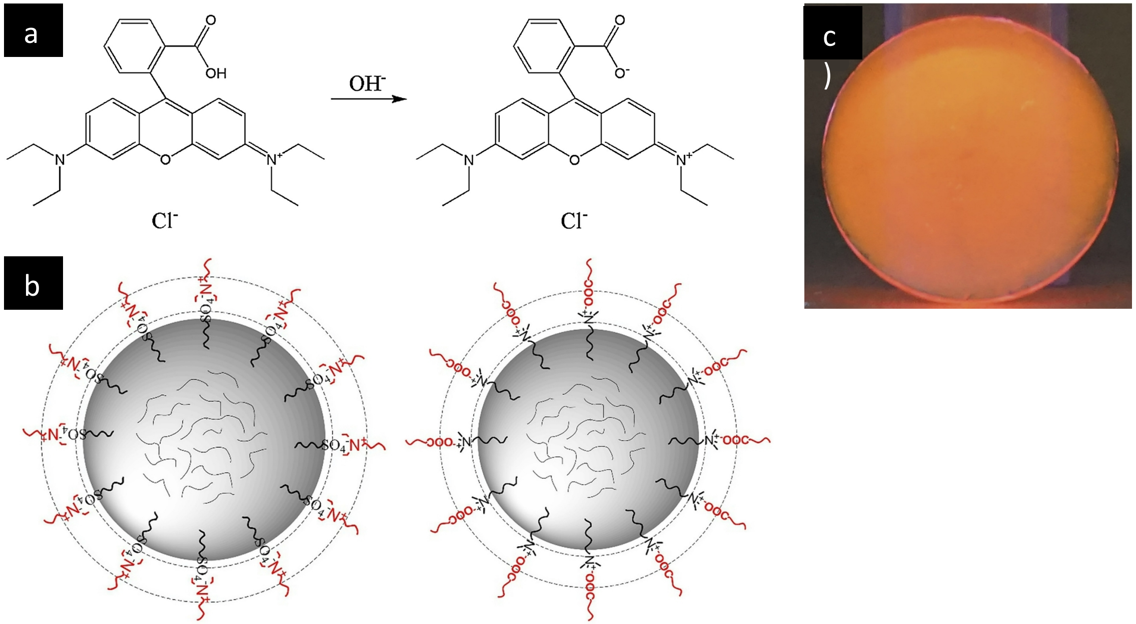
a
OH
OH^-
O^-
N
N^+
O
Cl^-
Cl^-
b
SO_4
N^+
OOC
c
)

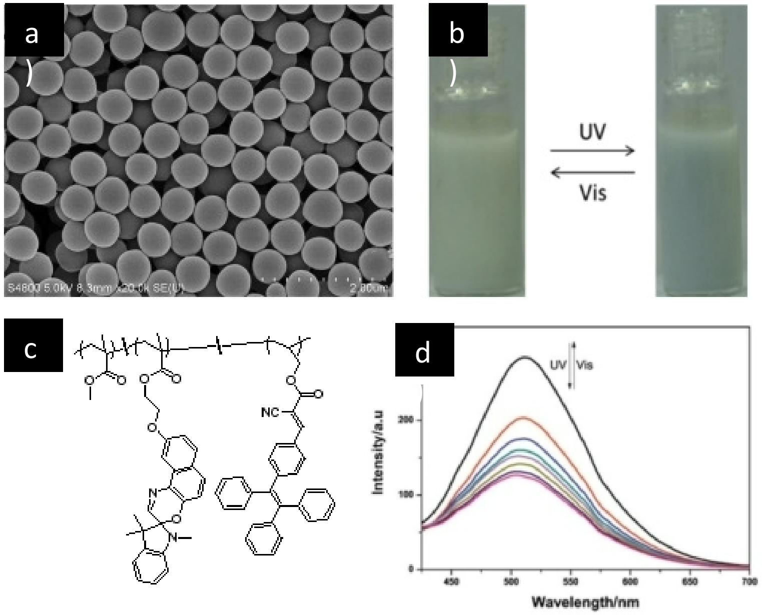
a
)
S4800 5.0kV 8.3mm x20.0k SE(U)
2.00um
b
)
UV
Vis
c
NC
N
O
N
d
UV
Vis
Intensity/a.u
200
100
0
450
500
550
600
650
700
Wavelength/nm

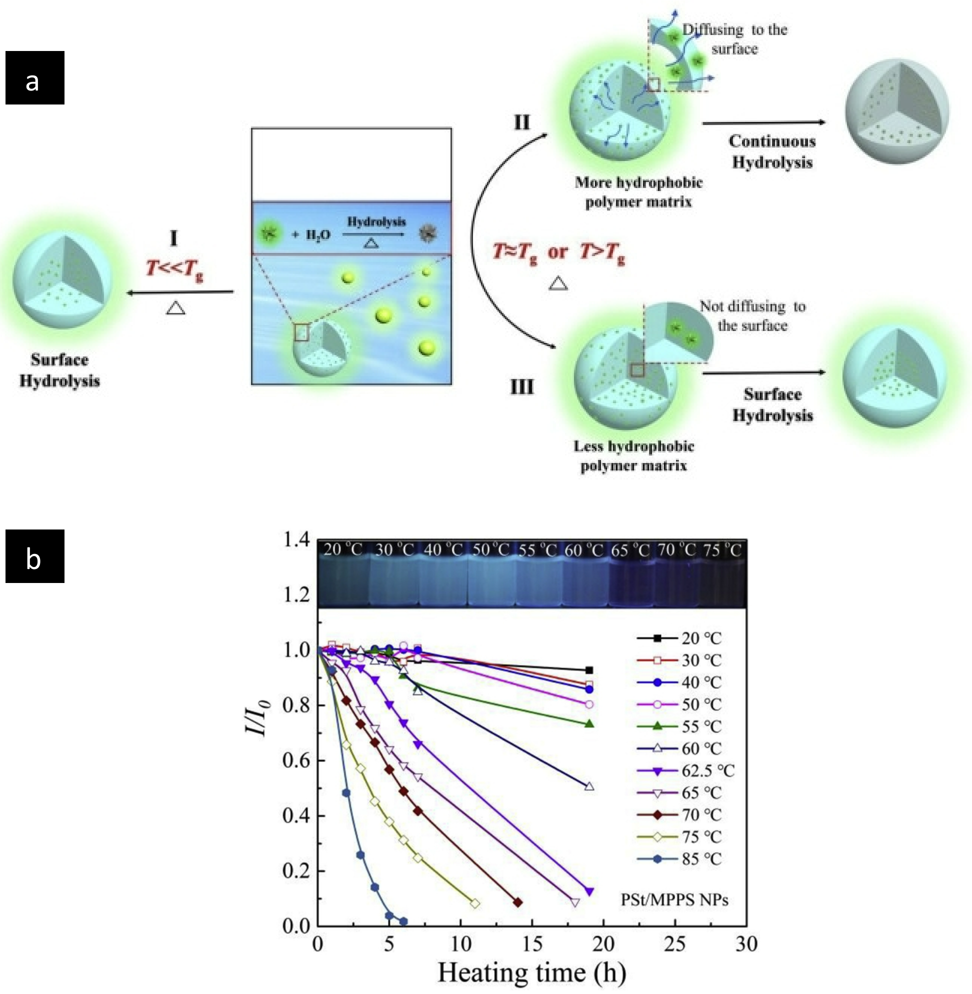
a
Hydrolysis
+ H2O
△
I
T<<Tg
△
Surface Hydrolysis
II
T≈Tg or T>Tg
△
III
Diffusing to the surface
More hydrophobic polymer matrix
Continuous Hydrolysis
Not diffusing to the surface
Less hydrophobic polymer matrix
Surface Hydrolysis
b
20 °C 30 °C 40 °C 50 °C 55 °C 60 °C 65 °C 70 °C 75 °C
I/I0
1.4
1.2
1.0
0.8
0.6
0.4
0.2
0.0
0
5
10
15
20
25
30
Heating time (h)
20 °C
30 °C
40 °C
50 °C
55 °C
60 °C
62.5 °C
65 °C
70 °C
75 °C
85 °C
PSt/MPPS NPs

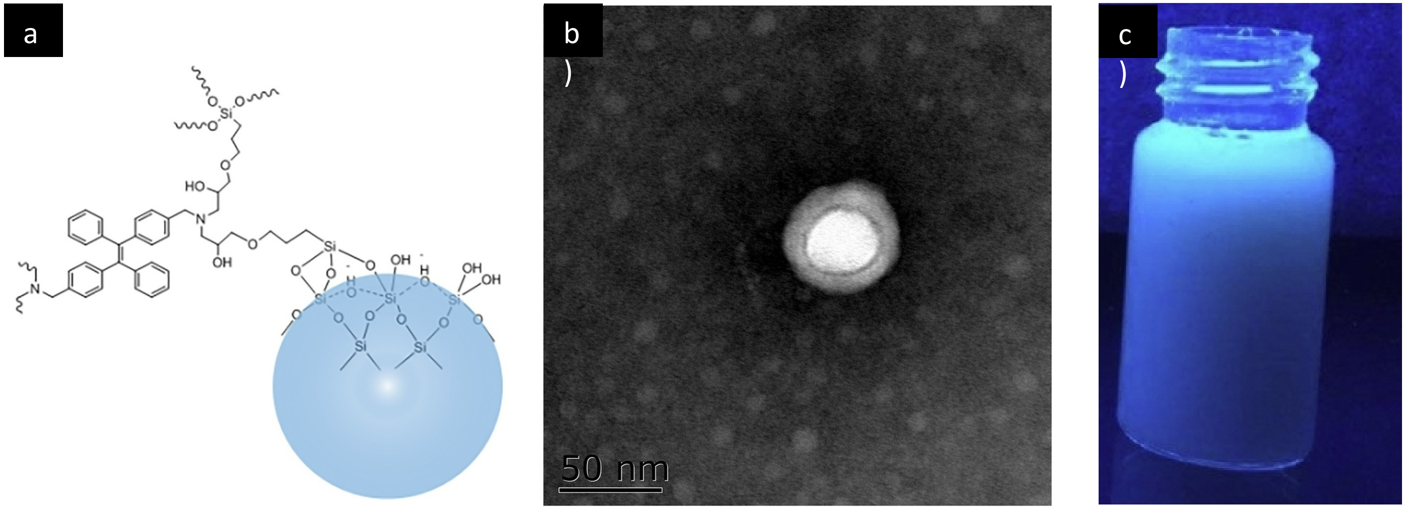
a
Si
O
HO
OH
N
OH
H
b
)
50 nm
c
)

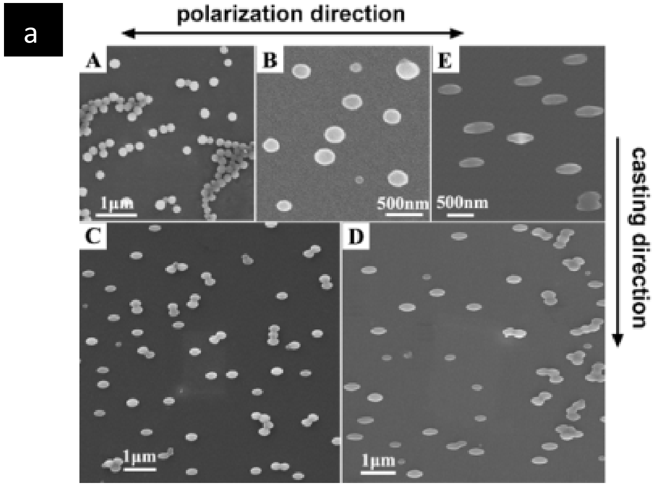
a
polarization direction
A
1μm
B
500nm
E
500nm
C
1μm
D
1μm
casting direction

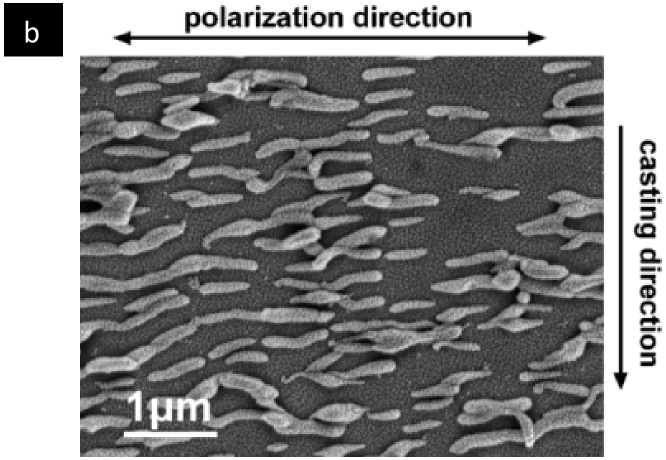
b
polarization direction
casting direction
1μm

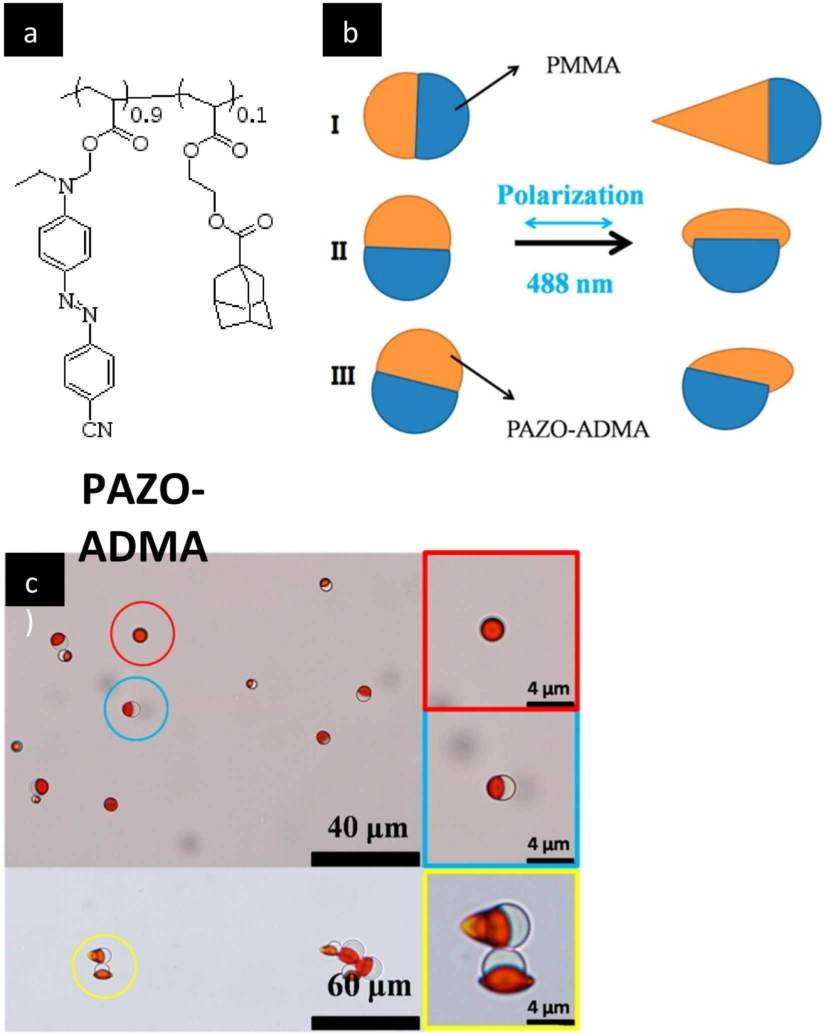
a
0.9
0.1
O
O
O
O
O
O
N
N
N
CN
PAZO-ADMA
b
PMMA
I
II
III
Polarization
488 nm
PAZO-ADMA
c
)
40 µm
60 µm
4 µm
4 µm
4 µm

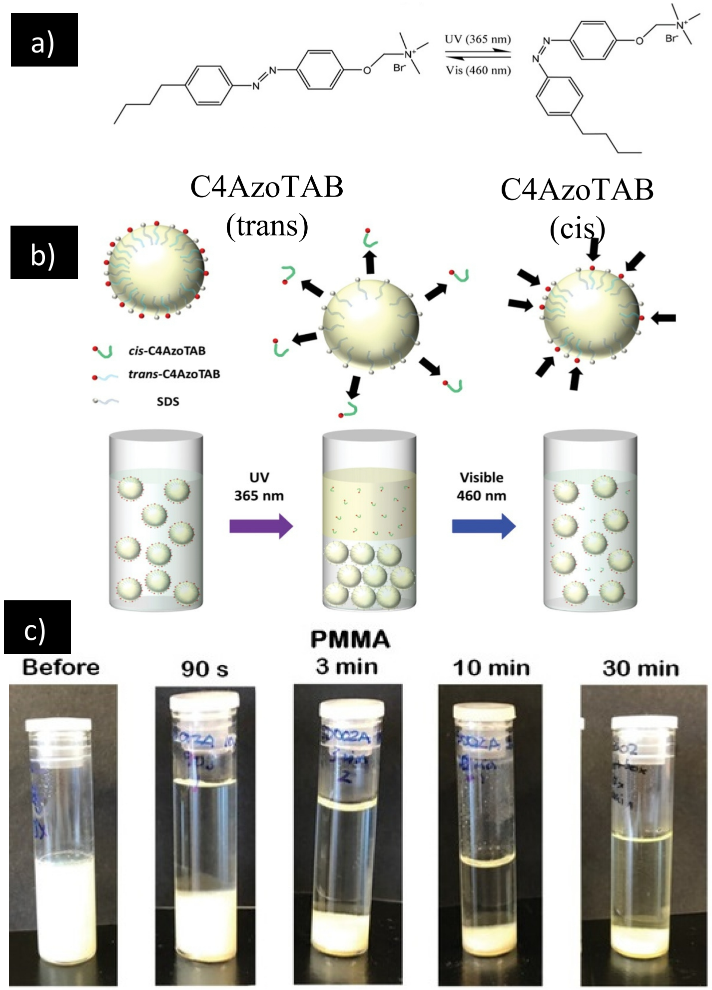
a)
UV (365 nm)
Vis (460 nm)
N
N
O
N+
Br-
C4AzoTAB (trans)
C4AzoTAB (cis)
b)
cis-C4AzoTAB
trans-C4AzoTAB
SDS
UV 365 nm
Visible 460 nm
c)
PMMA
Before
90 s
3 min
10 min
30 min

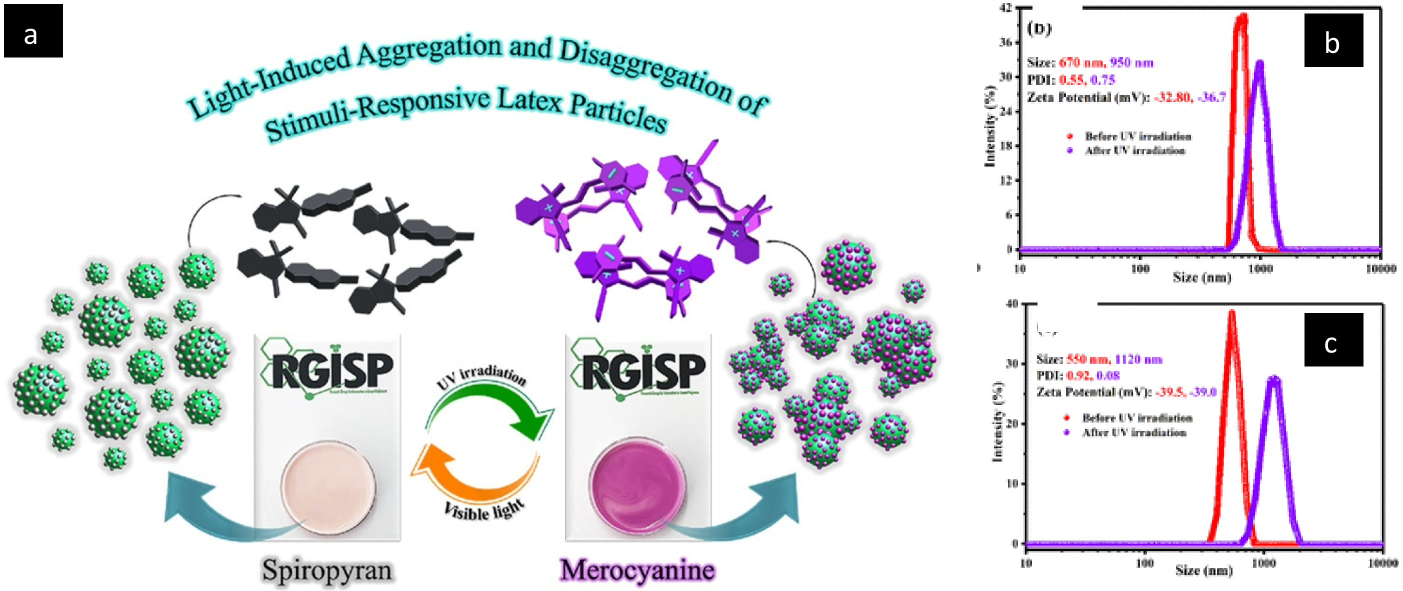
a
Light-Induced Aggregation and Disaggregation of Stimuli-Responsive Latex Particles
RGISP
UV irradiation
Visible light
RGISP
Spiropyran
Merocyanine
b
(b)
Size: 670 nm, 950 nm
PDI: 0.55, 0.75
Zeta Potential (mV): -32.80, -36.7
Before UV irradiation
After UV irradiation
Intensity (%)
0
6
12
18
24
30
36
42
10
100
1000
10000
Size (nm)
c
Size: 550 nm, 1120 nm
PDI: 0.92, 0.08
Zeta Potential (mV): -39.5, -39.0
Before UV irradiation
After UV irradiation
Intensity (%)
0
10
20
30
40
10
100
1000
10000
Size (nm)

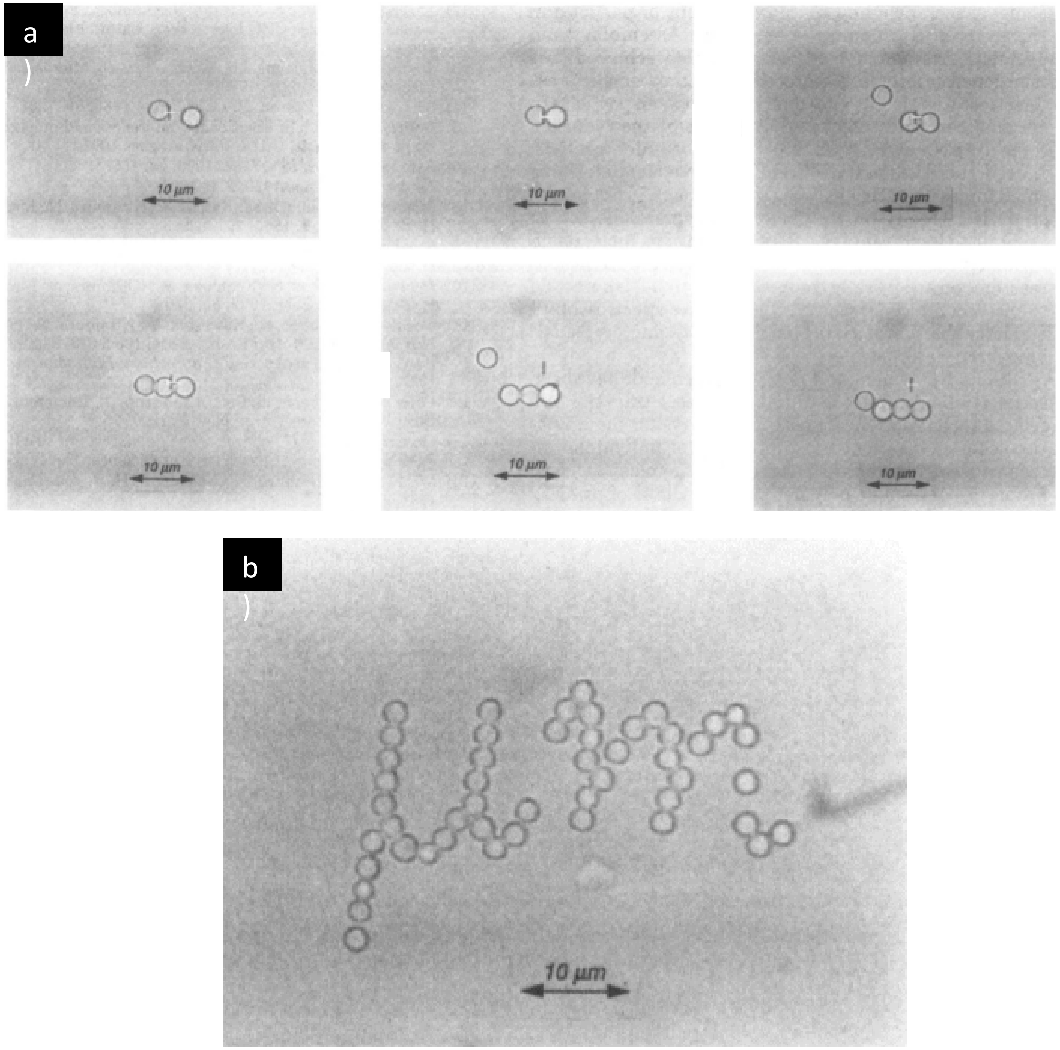
a)
10 µm
10 µm
10 µm
10 µm
10 µm
10 µm
b)
10 µm

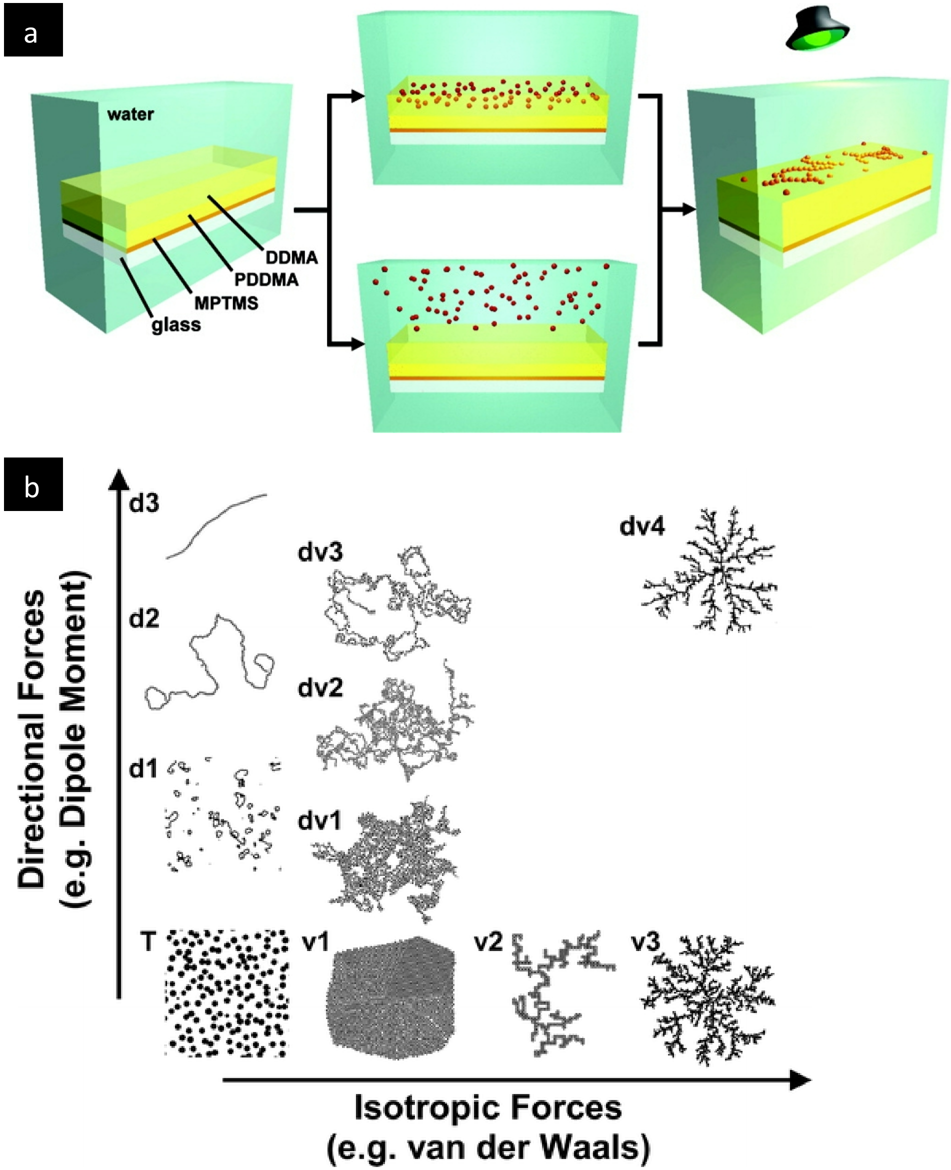
a
water
DDMA
PDDMA
MPTMS
glass
b
Directional Forces
(e.g. Dipole Moment)
d3
d2
d1
dv3
dv2
dv1
dv4
T
v1
v2
v3
Isotropic Forces
(e.g. van der Waals)

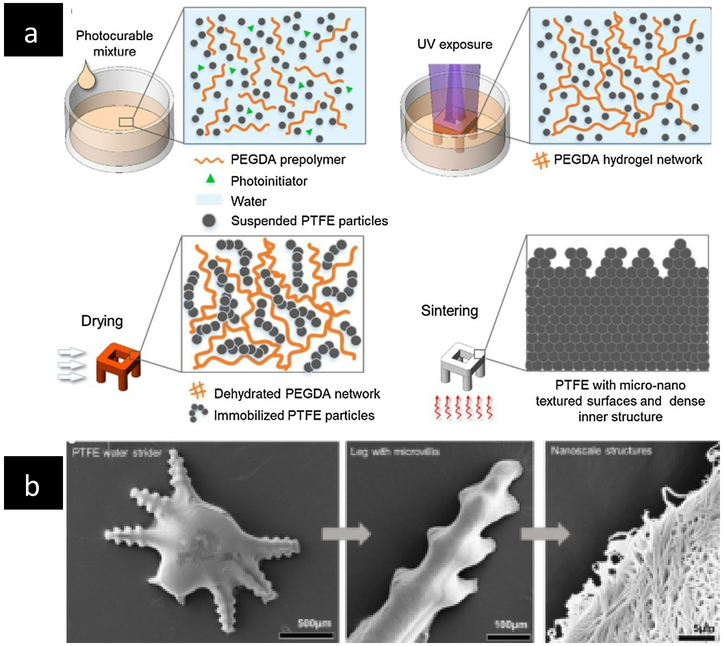
a
Photocurable mixture
PEGDA prepolymer
Photoinitiator
Water
Suspended PTFE particles
UV exposure
PEGDA hydrogel network
Drying
Dehydrated PEGDA network
Immobilized PTFE particles
Sintering
PTFE with micro-nano textured surfaces and dense inner structure
b
PTFE water strider
500μm
Leg with microvillis
100μm
Nanoscale structures
5μm

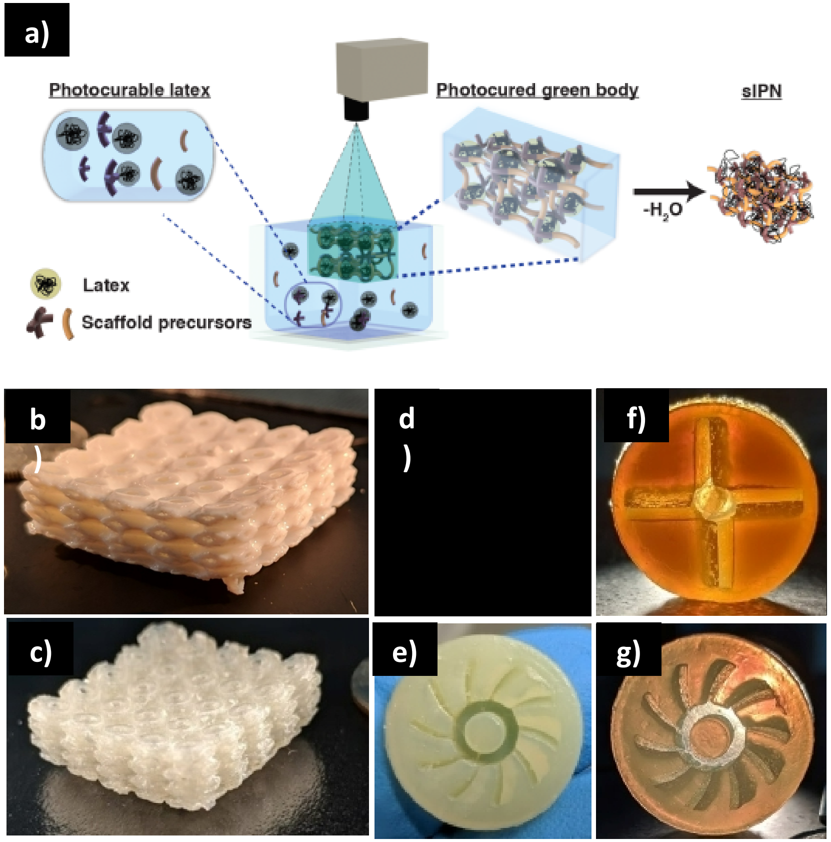
a)
Photocurable latex
Photocured green body
sIPN
-H$_2$O
Latex
Scaffold precursors
b)
d)
f)
c)
e)
g)

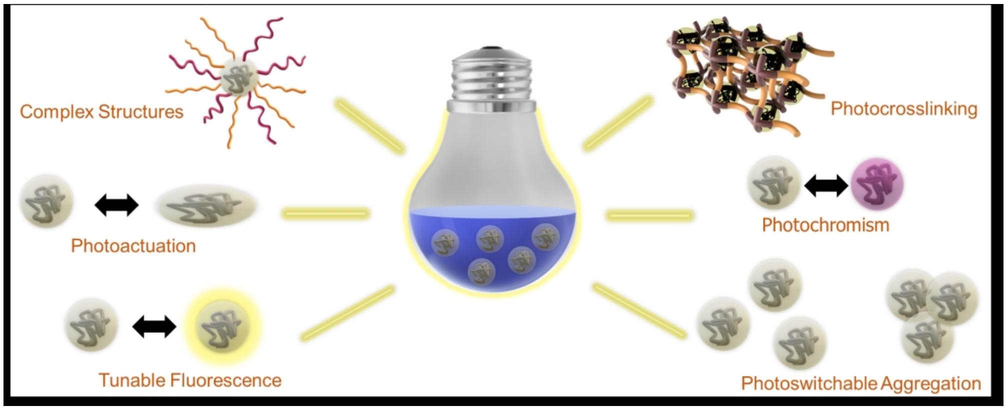

338x136mm (149 x 149 DPI)